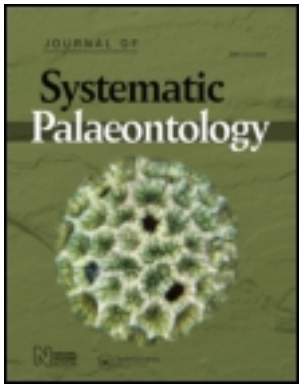

Journal of Systematic Palaeontology
Publication details, including instructions for authors and subscription information:
http://www.tandfonline.com/loi/tjsp20

The skull and neck of a new flagellicaudatan sauropod from the Morrison Formation and its implication for the evolution and ontogeny of diplodocid dinosaurs

Emanuel Tschopp[a] & Octávio Mateus[a]

[a] Faculdade de Ciências e Tecnologia- CICEGe, Universidade Nova de Lisboa, Monte de Caparica, Portugal; Museu da Lourinhã,&break; Rua João Luís de Moura 95,, Lourinhã, Portugal, 2530-158

Published online: 14 Dec 2012.

To cite this article: Emanuel Tschopp & Octávio Mateus (2013) The skull and neck of a new flagellicaudatan sauropod from the Morrison Formation and its implication for the evolution and ontogeny of diplodocid dinosaurs, Journal of Systematic Palaeontology, 11:7, 853-888, DOI: 10.1080/14772019.2012.746589

To link to this article: http://dx.doi.org/10.1080/14772019.2012.746589

Journal of Systematic Palaeontology, 2013
Vol. 11, Issue 7, 853–888, http://dx.doi.org/10.1080/14772019.2012.746589

The skull and neck of a new flagellicaudatan sauropod from the Morrison Formation and its implication for the evolution and ontogeny of diplodocid dinosaurs

Emanuel Tschopp* and Octávio Mateus

Faculdade de Ciências e Tecnologia- CICEGe, Universidade Nova de Lisboa, Monte de Caparica, Portugal; Museu da Lourinhã, Rua João Luís de Moura 95, 2530-158, Lourinhã, Portugal

(Received 27 July 2011; accepted 7 February 2012; first published online 14 December 2012)

A new taxon of diplodocid sauropod, *Kaatedocus siberi* gen. et sp. nov., is recognized based on well-preserved cervical vertebrae and skull from the Morrison Formation (Kimmeridgian, Late Jurassic) of northern Wyoming, USA. A phylogenetic analysis places it inside Diplodocinae (Sauropoda: Flagellicaudata: Diplodocidae), as a sister taxon to a clade uniting *Tornieria africana* and the classical diplodocines *Barosaurus lentus* and *Diplodocus*. The taxon is diagnosed by a unique combination of plesiomorphic and derived traits, as well as the following unambiguous autapomorphies within Diplodocidae: frontals separated anteriorly by a U-shaped notch; squamosals restricted to the post-orbital region; presence of a postparietal foramen; a narrow, sharp and distinct sagittal nuchal crest; the paired basal tuber with a straight anterior edge in ventral view; anterior end of the prezygapophyses of mid- and posterior cervical vertebrae is often an anterior extension of the pre-epipophysis, which projects considerably anterior to the articular facet; anterodorsal corner of the lateral side of the posterior cervical vertebrae marked by a rugose tuberosity; posterior margin of the prezygapophyseal articular facet of posterior cervical vertebrae bordered posteriorly by conspicuous transverse sulcus; posterior cervical neural spines parallel to converging. The inclusion of *K. siberi* and several newly described characters into a previously published phylogenetic analysis recovers the new taxon as basal diplodocine, which concurs well with the low stratigraphical position of the holotype specimen. *Dinheirosaurus* and *Supersaurus* now represent the sister clade to *Apatosaurus* and Diplodocinae and therefore the most basal diplodocid genera. The geographical location in the less known northern parts of the Morrison Fm., where *K. siberi* was found, corroborates previous hypotheses on faunal provinces within the formation. The probable subadult ontogenetic stage of the holotype specimen allows analysis of ontogenetic changes and their influence on diplodocid phylogeny.

http://zoobank.org/urn:lsid:zoobank.org:pub:70181793-AA2D-4F14-BAD2-F12B9D095B3D

Keywords: *Kaatedocus siberi*; new genus; Morrison Formation; Howe Quarry

Introduction

Diplodocids were most abundant and diverse during the Late Jurassic. Many specimens have been found in the USA, Portugal, Tanzania and possibly Asia (McIntosh 1990; Upchurch *et al.* 2004a; Upchurch & Mannion 2009; Mannion *et al.* 2012; Whitlock 2011a). The taxa of Late Jurassic Diplodocidae usually considered valid are: *Apatosaurus ajax* Marsh, 1877 (type species), *A. excelsus* (Marsh, 1879), *A. louisae* Holland, 1915, *A. parvus* (Peterson & Gilmore, 1902), *Barosaurus lentus* Marsh, 1890, *Dinheirosaurus lourinhanensis* Bonaparte & Mateus, 1999, *Diplodocus longus* Marsh, 1878 (type species), *D. carnegii* Hatcher, 1901, *D. hayi* Holland, 1924, *D. halli* (Gillette, 1991), *Supersaurus vivianae* Jensen, 1985, *Tornieria africana* (Fraas, 1908), and probably *Dyslocosaurus polyonychius* McIntosh *et al*., 1992 (McIntosh 1990; Upchurch *et al*. 2004a, b; Lucas *et al*. 2006). Most of these come from the Morrison Formation of southern Wyoming, Colorado or Utah, and only few skeletons are known from other parts of the world, even from northern Wyoming or Montana. The American Museum of Natural History, New York (AMNH) conducted one of their most productive field seasons in the Morrison Formation in north central Wyoming (Brown 1935). According to Brown (1935), more than 3000 bones of primarily diplodocids were recovered from the Howe Quarry near Shell, Wyoming, but none of the specimens have since been properly described, and many of them were lost subsequently during a fire at the AMNH (Michelis 2004). The site was later abandoned and only reopened in 1990 by a team of the Sauriermuseum Aathal, Switzerland (Ayer 2000; Christiansen & Tschopp 2010). Among the several dozens of bones excavated in 1990 and 1991 was a well-preserved and partly articulated neck and associated skull bones including both braincase and rostral elements (Fig. 1; Ayer 2000; Michelis 2004). As

*Corresponding author. Email: tschopp.e@campus.fct.unl.pt

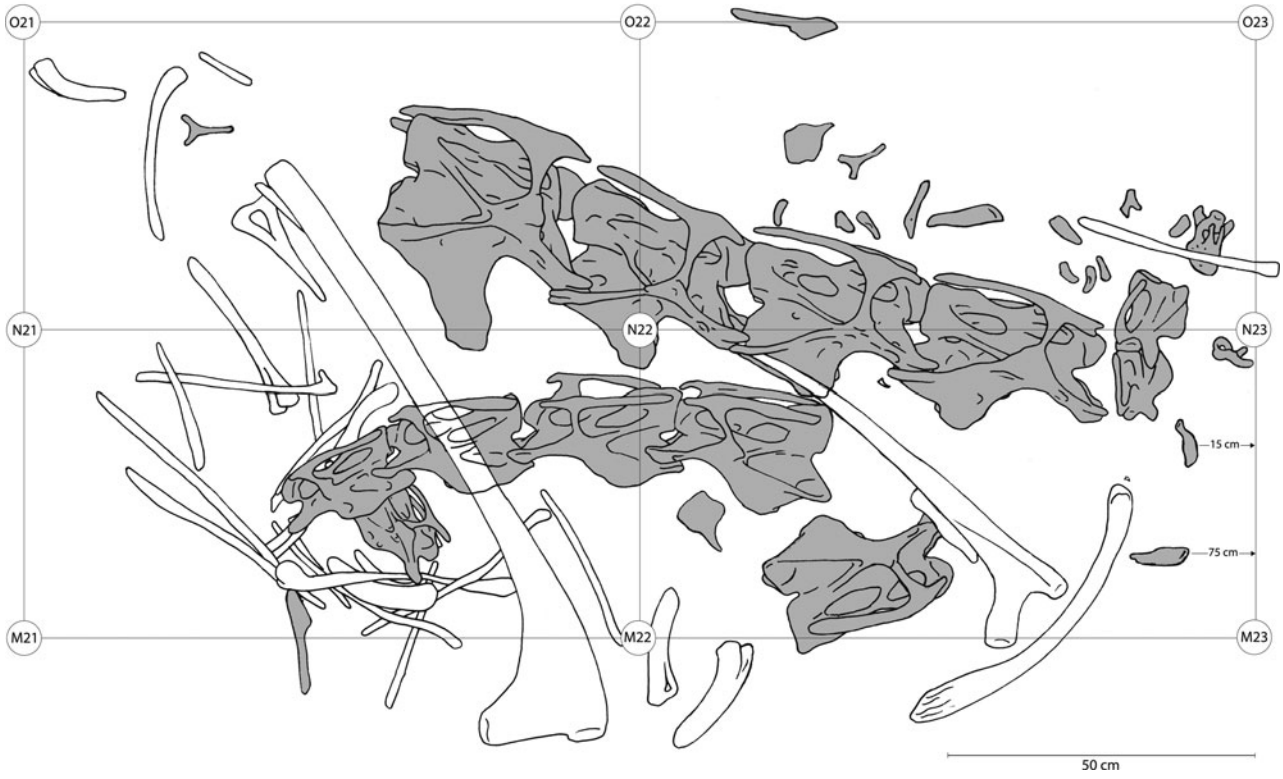

Figure 1. Quarry map of the holotype of *Kaatedocus siberi*, SMA 0004. Grey elements represent cervical vertebrae and disarticulated skull elements. Two of the latter were found 15 and 75 cm to the right of this grid (see arrows on the lower right side). SMA 0004 was associated with dorsal ribs, an interclavicle, sternal ribs and chevrons of maybe another individual. Drawing by Esther Premru. Scale bar = 50 cm.

the specimen (SMA 0004, nicknamed 'HQ 2') is relatively small, it was usually considered to be a juvenile *Diplodocus* (Ayer 2000), or *Barosaurus* (Michelis 2004). The present, detailed study of the morphology of SMA 0004 revealed that it can be clearly distinguished from both of these classical Late Jurassic diplodocines (see below). The new taxon thereby increases both the taxonomic and morphological diversity in the Morrison Formation.

Geological setting

The members of the Morrison Formation, as identified further south, are difficult to recognize in northern Wyoming. The only layer that has been used for stratigraphical correlation between the Howe Quarry and the various quarries in southern Wyoming, Colorado, Utah, South Dakota, Oklahoma and New Mexico is a clay change that was interpreted to divide the Morrison Formation into lower and upper parts (Turner & Peterson 1999; but see Trujillo 2006 for critiques). Such a clay change is present approximately 20 m above the Howe Quarry (Fig. 2). If Turner & Peterson (1999) prove to be right in interpreting this geological marker as useful for long distance correlation of the sites in the Morrison Formation, the Howe Quarry would be among the stratigraphically oldest fossil sites of the entire Morrison Formation (Turner & Peterson 1999; J. Ayer pers. comm. 2005). However, several authors propose a higher stratigraphical position for the Howe Quarry (Dodson *et al*. 1980; Swierc & Johnson 1996; Wilborn 2008). Swierc & Johnson (1996) dated the Howe Quarry as being 145.7 Ma, but this date groups all of the sites on the Howe Ranch together and does not take into account that the different quarries are situated at varying stratigraphical levels (see Fig. 2). Kvale *et al.* (2001) interpreted a second site approximately 10 m higher in stratigraphy (Howe-Stephens Quarry, see Schwarz *et al*. 2007b; Christiansen & Tschopp 2010) as being of 147 Ma in age. This implies a latest Kimmeridgian to earliest Tithonian age for the Howe Quarry.

Due to the fact that SMA 0004 is the first specimen of the Howe Quarry to be properly described and identified, previous synopses of the faunal assemblage of the site have to be regarded as provisional. An updated list of reported dinosaurs includes the sauropods *Camarasaurus*, *Apatosaurus*, *Kaatedocus* and possibly *Diplodocus* and *Barosaurus* (if they do not prove to be *Kaatedocus* as well), the theropods *Allosaurus* and a smaller taxon

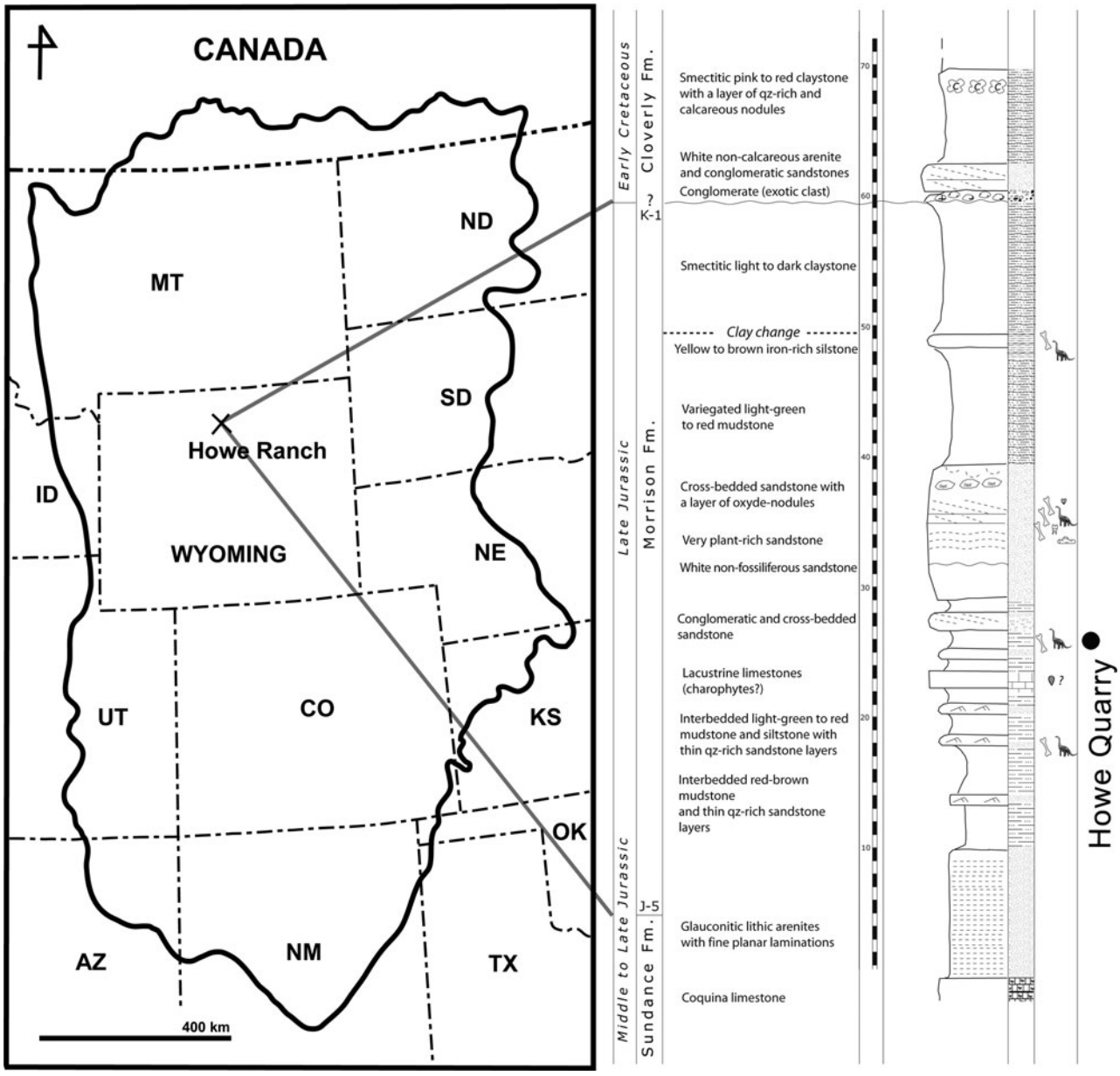

Figure 2. Geographical and geological setting of the Howe Quarry within the Upper Jurassic Morrison Formation. The Howe Quarry is located in North Central Wyoming, and stratigraphically well below the clay change. Modified from Schwarz *et al.* (2007b).

(represented by footprints and shed teeth), and the ornithopod *Camptosaurus* (Brown 1935; Foster 1998; Michelis 2004). Non-dinosaurian remains include carbonized wood fragments and a dental plate of the dipnoid fish *Ceratodus robustus* (Foster 1998; Michelis 2004).

Abbreviations

Institutional abbreviations

AMNH: American Museum of Natural History, New York, NY, USA; **ANS**: Academy of Natural Sciences, Philadelphia, PA, USA; **BYU**: Brigham Young University, Vertebrate Paleontology Collection, Provo, UT, USA; **CM**: Carnegie Museum of Natural History, Pittsburgh, PA, USA; **CMC**: Cincinnati Museum Center, Cincinnati, OH, USA; **DMNS**: Denver Museum of Nature and Science, Denver, CO, USA; **GMNH**: Gunma Museum of Natural History, Gunma, Japan; **HMNS**: Houston Museum of Nature and Science, Houston, TX, USA; **MB.R.**: Museum für Naturkunde, Berlin, Germany; **ML**: Museu da Lourinhã, Portugal; **SMA**: Sauriermuseum Aathal, Switzerland; **SNMB**: Staatliches Naturhistorisches Museum, Braunschweig, Germany; **UCL**: University College, London,

UK; **USNM**: United States National Museum, Washington, DC, USA; **WDC**: Wyoming Dinosaur Center, Thermopolis, WY, USA; **YPM**: Yale Peabody Museum, New Haven, CT, USA.

Anatomical abbreviations

a: articular; **acf**: anterior condyle fossa; **acdl**: anterior centrodiapophyseal lamina; **adt**: anterodorsal tuberosity; **apf**: anterior pneumatic foramen; **at**: atlas; **aof**: antorbital fenestra; **avl**: anteroventral lip; **ax**: axis; **bns**: bifid neural spine; **bpr**: basipterygoid process; **bt**: basal tuber; **bc**: braincase; **bo**: basioccipital; **cdf**: centrodiapophyseal fossa; **cpr**: crista prootica; **cprf**: centroprezygapophyseal fossa; **cprl**: centroprezygapophyseal lamina; **d**: dentary; **dp**: diapophysis posterior process; **epi**: epipophysis; **ex**: exoccipital; **f**: frontal; **fm**: foramen magnum; **int sprl**: interrupted spinoprezygapophyseal lamina; **la**: lacrimal; **ls**: laterosphenoid; **lsc**: lateral spine cavity; **ltf**: laterotemporal fenestra; **lprzc**: lateral prezygapophyseal cavity; **mt**: median tubercle; **m**: maxilla; **n**: external nares; **nc**: neural canal; **o**: orbit; **os**: orbitosphenoid; **p**: parietal; **pap**: parapophysis; **paof**: preantorbital fossa; **par bns**: parallel bifurcated neural spine; **pcdl**: posterior centrodiapophyseal lamina; **pl**: pleurocoel; **pm**: premaxilla; **po**: postorbital; **podl**: postzygodiapophyseal lamina; **poz**: postzygapophysis; **popr**: paroccipital process; **ppf**: posterior pneumatic fossa; **ppfo**: postparietal foramen; **prz**: prezygapophysis; **pra**: proatlas; **prcdf**: prezygapophyseal centrodiapophyseal fossa; **prdl**: prezygodiapophyseal lamina; **pre**: pre-epipophysis; **pro**: prootic; **prsl**: prespinal lamina; **ptf**: posttemporal fenestra; **pts**: prezygapophysis transverse sulcus; **pvf**: posteroventral flanges; **q**: quadrate; **qj**: quadratojugal; **sdf**: spinodiapophyseal fossa; **so**: supraoccipital; **sprl**: spinoprezygapophyseal lamina; **sprl ab**: spinoprezygapophyseal lamina anterior bulge; **spof**: spinopostzygapophyseal fossa; **spol**: spinopostzygapophyseal lamina; **sq**: squamosal; **tpol**: interpostzygapophyseal lamina; **tprl**: interprezygapophyseal lamina; **vk**: ventral keel; **vmc**: ventral median constriction.

Systematic palaeontology

Dinosauria Owen, 1842
Sauropoda Marsh, 1878
Eusauropoda Upchurch, 1995
Neosauropoda Bonaparte, 1986
Diplodocoidea Marsh, 1884 (see Upchurch 1995)
Flagellicaudata Harris & Dodson, 2004
Diplodocidae Marsh, 1884
Kaatedocus gen. nov.

Type species. *Kaatedocus siberi* sp. nov.

Diagnosis. See diagnosis for type and only species below.

Kaatedocus siberi gen. et sp. nov.
(Figs 3–10; see also Online Supplementary Material)

Diagnosis. Diplodocid sauropod with the following features not found in other sauropods: U-shaped notch separating the frontals anteriorly (Fig. 5); a rugose tuberosity that marks the anterodorsal corner of the lateral surface of the posterior cervical vertebrae (Fig. 10); posterior margin of the prezygapophyseal articular facet of posterior cervical vertebrae bordered posteriorly by a conspicuous transverse sulcus, separating the facet from the prezygapophyseal process (Fig. 10).

The following features are unique to *Kaatedocus* among Flagellicaudata or more inclusive clades: squamosals are restricted to the post-orbital region (unique for Diplodocoidea; Fig. 3); a straight anterior margin of the paired basal tuber in ventral view; anterior end of the prezygapophyses in mid- and posterior cervical vertebrae is formed by an accessory ventral process of the pre-epipophysis, that projects considerably anterior to the prezygapophyseal articular facet (Fig. 9).

The following features are unique to *Kaatedocus* among Diplodocidae: postparietal foramen present (Fig. 6); narrow, sharp and distinct sagittal nuchal crest on the supraoccipital (Figs 5, 6); and the narrowly diverging to subparallel posterior cervical neural spines (Fig. 10).

Furthermore, the new taxon can be distinguished from adult *Apatosaurus* and *Diplodocus* by its closed or very reduced preantorbital fenestra (Fig. 4); the dorsal portion of lateral edge of the lacrimal that bears a dorsoventrally short laterally projecting spur (Fig. 6); the relatively rounded snout (Fig. 5); a second small fossa in the quadrate, medially at the base of the pterygoid ramus; and the ratio of length/maximum basal diameter of the basipterygoid processes being less than four. In contrast to *Apatosaurus*, *Kaatedocus* exhibits spinoprezygapophyseal lamina that are reduced to a ridge, or totally interrupted at the base of the prezygapophysis of anterior and mid-cervical vertebrae (Figs 7, 8). *Kaatedocus* is different from *Diplodocus* due to the presence of at least 12 maxillary and dentary teeth that are not restricted to the anteriormost part of the jaw (Fig. 3). It can be distinguished from *Diplodocus*, *Tornieria* and *Barosaurus* due to its relatively short mid-cervical centra (Elongation Index (EI) = centrum length/height of posterior cotyle < 4).

Etymology. 'Kaate' means small in the Crow (Absaroka) language, one of the Native American tribes of northern Wyoming. 'Docus' is an allusion to *Diplodocus* and the Greek dokos/δοκος 'beam'. '*Siberi*' is after Hans-Jakob 'Kirby' Siber, b. 1942, doctor honoris causa of the University of Zurich, Switzerland. Siber is the founder and director of the Sauriermuseum Aathal, Switzerland, and organized and funded the excavation, preparation and curation of the holotype specimen of *Kaatedocus siberi*.

Holotype. SMA 0004: partial skull (right premaxilla, both maxillae, left lacrimal, both frontals, both postorbitals, both

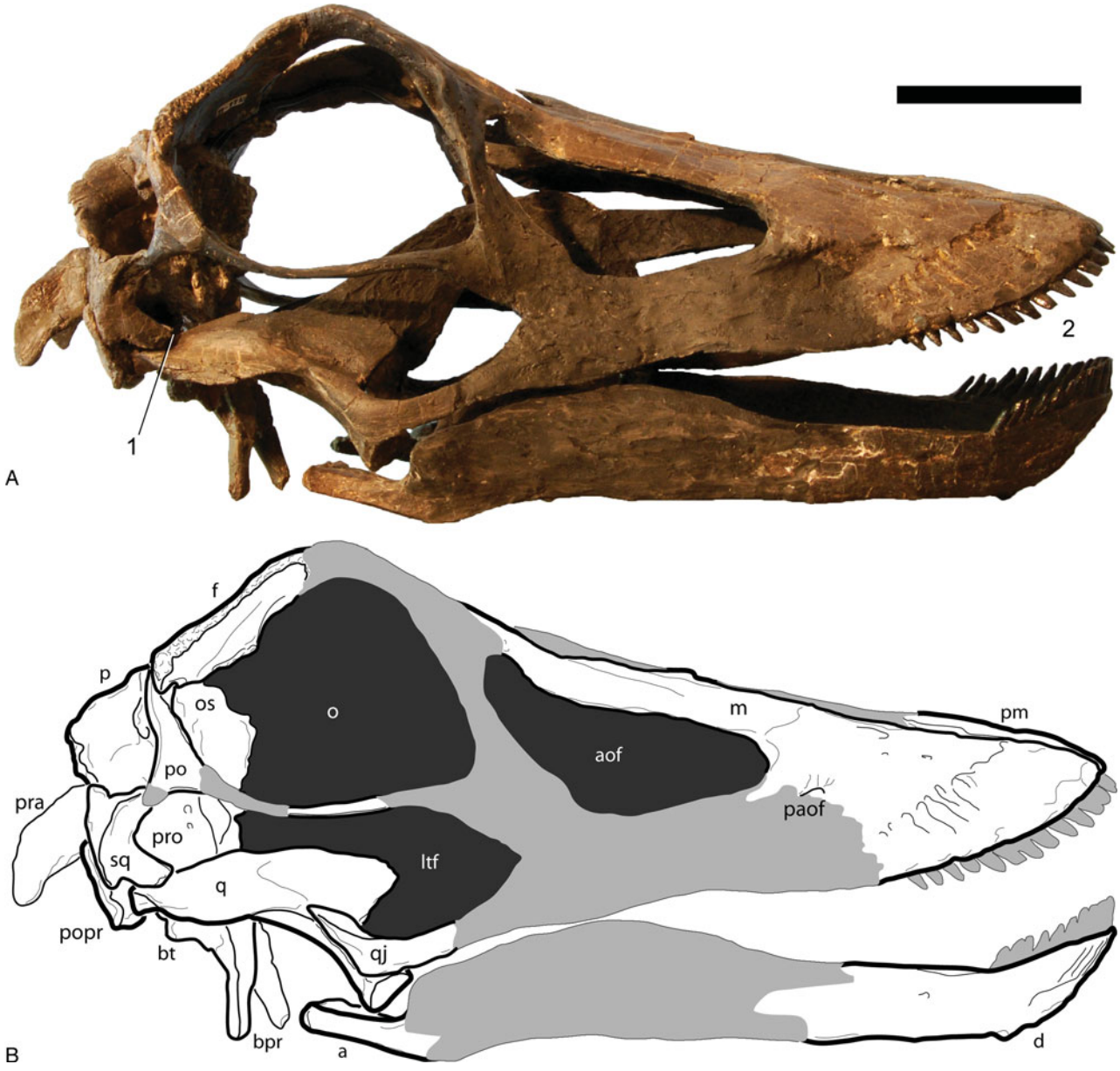

Figure 3. A, Photograph and **B,** drawing of the reconstructed skull of the holotype of *Kaatedocus siberi* (SMA 0004) in right lateral view. Light grey areas in B are reconstructed parts. The right surangular is mistakenly mounted as left angular. Notes corresponding to diagnostic features: (1) anteriorly restricted squamosal; (2) high tooth count, teeth not restricted to anteriormost jaw. Scale bar = 5 cm.

quadratojugals, both quadrates, both squamosals, both parietals, complete braincase, both dentaries, right surangular, both articulars (Figs 3–6, Online Supplementary Material), and cervical series from proatlas to cervical vertebra 14 (Figs 7–10 and Online Supplementary Material).

The only elements that were not found articulated are one proatlantal element and the axis. They were included in the mount as they fit in size and morphology. The assignment of the axis to the holotype is provisional pending the discovery of a second specimen including this element. However, as no character in the phylogenetic analysis used herein describes axial morphology, the attribution of these elements to the holotype does not affect the phylogenetic position of *Kaatedocus siberi*.

Locality and horizon. SMA 0004 was recovered from the Howe Quarry in the vicinity of Shell, Bighorn County, north-central Wyoming, USA (44° 40′ 2.95″ N/107° 49′ 8.12″ W). The site is interpreted to be of Late Kimmeridgian or Early Tithonian age, in the upper part of the lower Morrison Formation (Fig. 2; Schwarz *et al.* 2007b; J. Ayer pers. comm. 2005).

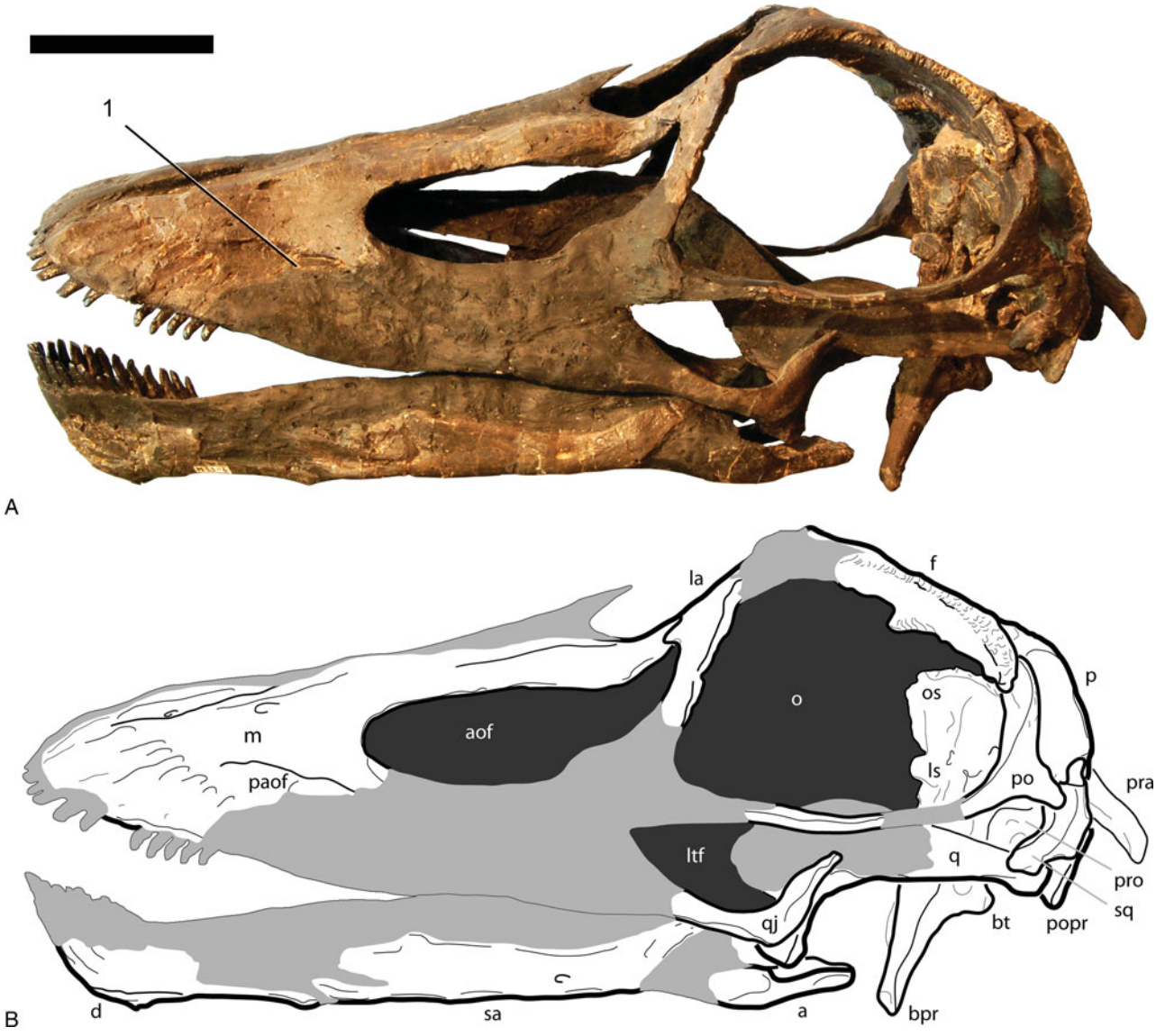

Figure 4. A, Photograph and **B,** drawing of the reconstructed skull of the holotype of *Kaatedocus siberi* (SMA 0004) in left lateral view. Light grey areas in B are reconstructed parts. The right surangular is mistakenly mounted as left angular. Note corresponding to diagnostic features: (1) closed or reduced preantorbital foramen. Scale bar = 5 cm.

Ontogeny. The ontogenetic stage of SMA 0004 is ambiguous as the specimen exhibits an intermediate morphology with osteological features that have been interpreted historically as indicators of either juvenile or adult ontogenetic stages.

Compared to other diplodocids, a young age is implied by the small size (combined skull and neck length approximately 3.8 m, estimated body length 14 m, based on intermediate cervical vertebrae elongation between *Apatosaurus* and *Diplodocus*) and the relatively large orbit. With a total length of 30 cm, the skull is slightly larger than the juvenile *Diplodocus* CM 11255, and reaches approximately 58% of the length of the adult *Diplodocus* skull CM 11161 (Holland 1906; Whitlock *et al*. 2010). In addition, the incomplete fusion of the parietals, the rounded muzzle (in contrast to the squared snout of adult *Diplodocus* and *Apatosaurus*), the restriction of the bifurcation of cervical neural spines to mid- and posterior cervical vertebrae, and relatively shorter cervical centra have recently been interpreted to be typical for a juvenile ontogenetic stage (Wedel *et al.* 2000; Whitlock *et al.* 2010; Woodruff & Fowler 2012). On the other hand, the complete co-ossification in all cervical vertebrae, and the presence of rugose tubercles, or roughened areas on laminae edges on both cranial and cervical elements indicate a higher ontogenetic age (Varricchio 1997; Ikejiri *et al*. 2005; Schwarz *et al.* 2007b).

Figure 5. A, Photograph and **B,** drawing of the reconstructed skull of the holotype of *Kaatedocus siberi* (SMA 0004) in dorsal view. Light grey areas in B are reconstructed parts. Notes corresponding to diagnostic features: (1) U-shaped frontal notch; (2) rounded snout; (3) narrow, distinct sagittal nuchal crest. Scale bar = 5 cm.

Taking all of the above mentioned features into account, the juvenile traits are generally seen as well on adult specimens of other taxa (like the more rounded snout of dicraeosaurids, or the less developed bifurcation of the cervical vertebrae in *Barosaurus*; Janensch 1935; McIntosh 2005), whereas the indicators for a subadult stage of SMA 0004 (in particular the advanced co-ossification and the conspicuous rugosities on both skull bones and vertebrae) are not reported from any specimens of young age, to our knowledge. In fact, adult alligators (Ikejiri 2012), and a juvenile *Allosaurus* (Birkemeier 2011) have recently been reported to possess open neurocentral sutures in cervical vertebrae, but fused centra and neural spines in caudal and/or dorsal elements. This indicates that neurocentral closure proceeds from the back to the front, with the cervical vertebrae being the last to co-ossify (Birkemeier 2011; Ikejiri 2012). On the other hand, the subadult flagellicaudatan *Suuwassea emilieae* ANS 21122 was reported to have fused cervical arches, but unfused mid-caudal vertebrae, which might contradict the developmental model supported by the above-mentioned taxa (Harris 2006c). However, based on the available material, we still interpret SMA 0004 as a subadult specimen that retained a small body size. This is in agreement with the

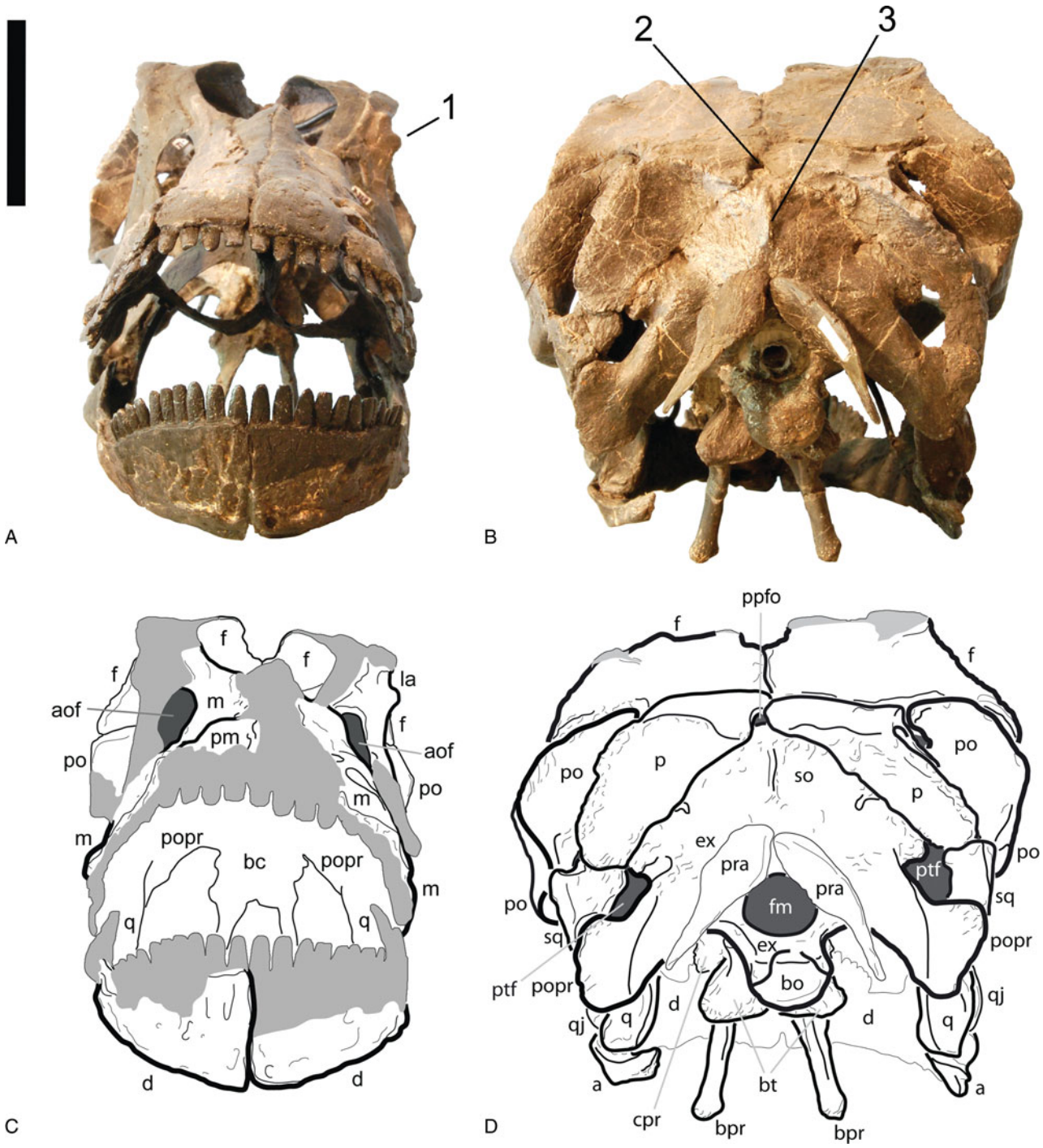

Figure 6. A, B, Photographs and **C, D,** drawings of the reconstructed skull of the holotype of *Kaatedocus siberi* (SMA 0004) in anteroventral (A, C), and posterodorsal (B, D) views. Light grey areas in C and D are reconstructed parts. Notes corresponding to diagnostic features: (1) lateral lacrimal spur; (2) postparietal foramen; (3) narrow, distinct sagittal nuchal crest. Scale bar = 5 cm.

ontogenetic stages as described for *Camarasaurus* in Ikejiri *et al.* (2005). According to these authors, neurocentral closure in cervical vertebrae, as well as the subdivision of cervical pleurocoels, happens in subadult to adult stages.

Description

Terminology follows the standard nomenclature generally used (anterior and posterior instead of cranial and caudal). For the names of the vertebral lamina and fossae, we

follow Wilson (1999) and Wilson *et al*. (2011), respectively, with two exceptions: instead of intrapre- and intrapostzygapophyseal lamina we use the terms interpre- and interpostzygapophyseal lamina, as the prefix inter- describes better the arrangement between the two zygapophyses. To keep confusion to a minimum we keep the abbreviations proposed by Wilson (1999): tprl (interprezygapophyseal lamina) and tpol (interpostzygapophyseal lamina). Other anatomical abbreviations used in the text are: CV (cervical vertebra), and EI (Elongation Index, ratio between the centrum length and the height of the posterior cotyle; Upchurch 1998).

Skull

The general shape of the skull is highly similar to *Diplodocus* or *Apatosaurus*, elongated and having a retracted external nares. Some obvious differences compared to adult skulls (e.g. AMNH 969, CM 11161, 11162, USNM 2672, 2673) include the larger orbit and the teeth that reach further backwards, although these are still restricted to the anteriormost part of the skull (Figs 3, 4).

Premaxilla. The right premaxilla preserves the anterior portion, lacking the anteriormost dorsal border and the teeth. The main body is simple, without a sinuous curve building a muzzle. It is broadest anteriorly, and its straight lateral and medial edges slightly converge posteriorly, including a very acute angle of approximately 10°. The dorsal surface does not bear any anteroventrally extending grooves as are present in *Dicraeosaurus hansemanni* MB.R.2337. Four alveoli are visible, oriented such that the teeth would be procumbent. There is no indication of an anterior dorsoventral expansion as in *Diplodocus* USNM 2673 or *Dicraeosaurus hansemanni* MB.R.2337.

Maxilla. Both maxillae lack their posteroventral ramus and teeth. From the main body, the lamina-like dorsal ramus projects posteriorly and tapers until it meets the lacrimal. Its ventral edge is convex, resulting in a concave dorsal border of the antorbital fenestra as in most diplodocid skulls (e.g. CM 3452, 11161, 11162, 11255; USNM 2672). Slightly lateral to the border with the premaxilla, both the subnarial and the anterior maxillary foramen are well visible and closely spaced. A third, small foramen is situated just lateroventrally of the subnarial foramen. The preantorbital fossa is a longitudinal depression marked by an acute step bordering it dorsally. Such a development has been considered autapomorphic for *Diplodocus* (Mannion *et al*. 2012), but there it roofs a relatively large preantorbital fenestra (e.g. CM 3452, 11161, 11255; Berman & McIntosh 1978; Whitlock *et al*. 2010; pers. obs. 2011), which is not present in SMA 0004. It does not open into a fenestra as in *Diplodocus* (e.g. CM 3452, 11161, 11255; Berman & McIntosh 1978). In this respect, *Kaatedocus siberi* is very similar to *Dicraeosaurus* (MB.R.2336; pers. obs. 2011), where a very reduced foramen-like opening is present in the posteriormost extension of a dorsally well-defined fossa. The posteriormost portion is not preserved in SMA 0004 and could also exhibit such a small opening. The rostral portion of the main body of the maxilla shows the wavy surface typical for the part containing the replacement teeth. At least 12 alveoli can be counted in the right element.

Quadratojugal. Only the posterior half of both quadratojugals has been preserved. They are L-shaped bones that cover the quadrate laterally with the shorter dorsal ramus, and would extend anteriorly to meet the jugal and the maxilla if preserved entirely. The two arms of the L are transversely compressed and form an angle of approximately 110°. The dorsal ramus projects dorsoposteriorly, as in *Diplodocus* or *Apatosaurus*, and curves slightly more backwards in its upper half. From there, it tapers to an acute tip, which does not extend far posteriorly, and thus remains well separated from the anteroventral projection of the squamosal – a typical feature in diplodocids, which is also present in *Suuwassea* (ANS 21122, pers. obs. 2011; contrary to the interpretation of Harris 2006a). The preserved portion of the anterior ramus is dorsoventrally shortest close to where it grades into the dorsal process, and expands slightly towards the anterior end.

Lacrimal. The left lacrimal preserves the dorsal part that articulates with the maxilla anteriorly, the nasal medially, and the prefrontal posteriorly. The anterior edge of the lacrimal is straight until it reaches the posterodorsalmost end of the antorbital fenestra. The posterior border becomes thicker towards the upper end, where it develops a concavity that holds the lacrimal foramen. Lateral to this foramen, the lacrimal develops a blunt bony spur projecting laterally, a feature that is only seen in the juvenile diplodocid skulls CM 3452 and 11255, but not in adults (CM 11161, 11162; Berman & McIntosh 1978; pers. obs. 2011).

Frontal. Both frontals are preserved completely. Anteroposterior length is about equal to maximum transverse width. The dorsal surface is flat and relatively smooth. The anterior and posterior margins are straight and subparallel at their medial portions. The lateralmost quarter of the anterior edge is marked by a distinct, acute V-shaped invagination that would receive the posterior process of the prefrontal, which does not extend far posteriorly as in *Diplodocus*, but remains well distant from the parietal. The posterior edge of the frontal also curves inward, but to a lesser degree than the anterior one. This indentation is gently rounded and forms the articulation facet for the dorsomedial process of the postorbital. The medial edges are straight along their posterior half and form an approximate right angle with the frontal–parietal suture. Anteriorly, they curve inwards, so that between the frontals a U-shaped notch develops. The edge is extremely thin, and neither exhibits any indication

of fracturing nor is undulose as sutures often are. The notch, therefore, either enclosed a posterior process of the nasals, having a straight suture, or remained open as a posterior extension of the external nares, so that the nasals did not contact each other medially. The only sauropod with a similar development is *Spinophorosaurus nigerensis*, which has a narrow, V-shaped notch between the frontals (Knoll *et al*. 2012). The wider, U-shaped notch of *Kaatedocus siberi* can thus be considered an unambiguous autapomorphy. The straight lateral margins contribute to a major part of the dorsal edge of the orbit, and exhibit a similar rugosity as is typical for bone sutures, present in most diplodocoid skulls (e.g. AMNH 969, 7530, CM 3452, MB.R.2386, 2387, pers. obs. 2011). This indicates the existence of a cartilaginous palpebral element (homologue to the ossified palpebral bones in ornithischian dinosaurs; see Maidment & Porro 2010). In ventral view it becomes clear that the frontal supports the end of the posterior process of the prefrontal from below. From there, a conspicuous, sharp ridge passes the ventral surface obliquely until it reaches the anterior end of the articulation surface for the anterodorsal part of the braincase, which is highly rugose and stands almost perpendicularly to this ridge.

Postorbital. Both postorbitals preserve their dorsomedial process and parts of the anterior process that forms the ventral border of the orbit. It covers the frontal posteriorly, and overlies the anterodorsalmost corner of the squamosal laterally. The left element also shows the posterior process. The dorsomedial process is relatively high dorsoventrally and compressed anteroposteriorly. It extends medially to reach the frontal–parietal suture, thereby excluding the frontal from the margin of the supratemporal fenestra. It is dorsoventrally convex posteriorly and concave anteriorly. The anterior process is a dorsoventrally compressed, subtle structure that extends nearly straight and subparallel to the dorsal margin of the orbit until it would reach the jugal, which is not preserved in SMA 0004. Posteriorly, the postorbital anterior process curves gently upwards, expanding slightly transversely. The posterior ramus is very short and acute. It projects almost straight posteriorly in dorsal view, and curves to a small degree ventrally in lateral aspect.

Parietal. Both parietals are complete and not fused. They contact the frontals anteriorly, the supraoccipital and exoccipital medioventrally, and the postorbitals and squamosals laterally. The parietals are dorsally flat bones on the posterior skull roof with a short anterolateral and a longer posterolateral process, which together enclose a major portion of the supratemporal fenestra. The frontal–parietal suture is more or less straight, and partly obscured due to the restoration and mounting of the skull, but appears to have been open in lifetime (B. Pabst pers. comm. 2011). There is no trace visible of a pineal foramen, which would be situated where the paired frontals and parietals meet. A postparietal foramen can be observed posteriorly between the parietals and the supraoccipital, similar to the condition in *Dicraeosaurus*, *Amargasaurus* and *Suuwassea* (Janensch 1935; Salgado & Bonaparte 1991; Harris 2006a; Whitlock 2011a). The medial borders of the parietals bend slightly laterally in their posterior half, somewhat anterior to where they meet the supraoccipital, which they overlap to a small degree. The posterior border of the dorsal portion of the parietals is transversely concave in dorsal view. From there, the posterolateral process extends in a right angle ventrally, and laterally, following the oblique dorsolateral edge of the supraoccipital, and forms the posterior margin of the supratemporal fenestra. The posterior aspect of this process has a subequal or greater surface area than the flat dorsal portion. It is anteroposteriorly compressed, dorsomedially–ventrolaterally convex, and dorsolaterally–ventromedially concave. The dorsal edge extends straight dorsomedially–ventrolaterally, so that the supratemporal fenestra faces somewhat posteriorly as well, unlike the condition in *Diplodocus* CM 3452, but similar to *Apatosaurus* CM 11162 (Berman & McIntosh 1978). The ventrolateral end of the posterolateral process is rounded and overlaps the squamosal laterally. The anterior surface gently curves into the anteroposteriorly concave medial side of the parietal, which is well separated by a distinct ridge from the dorsal flat area of the same bone. In its anterior part, it bears the short anterolateral process, which projects ventrolaterally forming the anterior edge of the supratemporal fenestra, together with the postorbital.

Squamosal. The squamosals are complete except for their dorsalmost part, which is not preserved on either side. It connects with the postorbital anterodorsally, with the quadrate anteroventrally, with the parietal dorsomedially, and with the paroccipital process posteroventrally. Dorsally, the squamosal forms the posterolateral corner of the supratemporal fenestra, ventromedially the dorsolateral edge of the posttemporal fenestra, and anteriorly the posteriormost corner of the infratemporal fenestra. It is a strongly transversely curved bone, with its convex side facing outwards, forming part of the posterolateral edge of the skull. In lateral view, the anterodorsal process of the squamosal bears a dorsoventral concavity for the reception of the postorbital. The ventral process tapers to a blunt tip that points slightly anteriorly as well, but does not exceed the posterior border of the orbit as in other diplodocoids (e.g. Berman & McIntosh 1978; Salgado & Bonaparte 1991). Both its anterior and posterior borders are straight, before they curve frontwards and backwards, respectively. In the posterior margin this happens slightly earlier, and the posterior process is thus dorsoventrally longer than the anterior ramus. The squamosal therefore bears a short posteroventral process but does not form such a distinct ‘prong’ as present in *Amargasaurus* (Salgado & Bonaparte

1991; Whitlock 2011a). In posterior view, the squamosals are dorsoventrally convex, with the dorsomedial process projecting medially to meet the parietal.

Quadrate. Both quadrates lack their anterodorsal portions of the wing-like anterodorsal ramus, but are otherwise complete. They are triradiate bones forming the jaw articulation with the articular ventrally, contacting the pterygoids anteromedially, and the squamosal posteriorly. The articular facet for the mandibular joint is subtriangular, lacking a medial process as the one seen in some rebbachisaurids (Mannion *et al*. 2012; Whitlock 2011a). It is located at the ventral end of the relatively stout ventral ramus, which is oriented at an angle of about 90° to the skull roof. The anteroventral projection of the quadrate shaft is covered laterally almost completely by the dorsal ramus of the quadratojugal, and exhibits a shallow concavity on its posterior side. This concavity extends onto the ventral side of the posterior process, forming a shallow quadrate fossa as in other diplodocids (Wilson 2002; Upchurch *et al.* 2004a). Posteriorly, the ramus tapers both in dorsoventral and in mediolateral directions. It curves slightly medially as well, so that the whole lateral side of the quadrate becomes anteroposteriorly slightly convex. The wing-like pterygoid flange is a very thin lamina originating at the lateral edge of the posterior ramus. Medially it borders another shallow fossa that lies on the quadrate shaft and becomes deeper anteriorly. Such a cavity has not been described in any diplodocid sauropod, and personal observations showed it to be absent in most diplodocid skulls (e.g. AMNH 969; CM 11161, 11162, 11255; USNM 2672, 2673). However, the possible *Diplodocus* skull CM 3452, as well as the quadrates assigned to the holotype of *Apatosaurus ajax* YPM 1860, show similar features.

Braincase and occiput

Supraoccipital and exoccipital-opisthotic complex. The supraoccipital is complete and well fused to the exoccipital–opisthotic complex so that sutures are difficult to observe. The whole fused element is subtriangular, touching the parietals anterolaterally, bordering the posttemporal fenestrae with the dorsolateral margin of the paroccipital processes, and contributing to the upper portion of the occipital condyle ventrally. It roofs the braincase posteriorly, encloses the foramen magnum, and bears two oblique, ellipsoid facets right dorsolaterally of the foramen magnum for the articulation with the wing-like proatlas. Together, these facets form an inverted V-shape and reproduce more or less the angle included by the paroccipital processes. Dorsal to these proatlantal facets, the supraoccipital bears a narrow sagittal nuchal crest, very similar to the state in *Suuwassea amilieae* ANS 21122 (Harris 2006a). This ridge extends dorsally to the dorsomedial, rounded corner of the supraoccipital, which also borders the postparietal foramen posteriorly. From here, the oblique dorsolateral borders extend ventrolaterally, bearing a short posttemporal process at their outer ends that meets the squamosal, and thereby excludes the parietal from the anterior margin of the posttemporal fenestra. Close to the dorsolateral border, at about midlength, there is a foramen like the one interpreted as an external occipital foramen in the *Apatosaurus* BYU 17096 (Balanoff *et al.* 2010). Another small foramen is situated between the latter and the proatlas facets, near the base of the paroccipital process.

The paroccipital processes are anteroposteriorly flat structures that project ventrolaterally, and slightly posteriorly to meet the squamosal and the quadrate. Their dorsal and ventral margins are subparallel in posterior view, and also parallel to a line projecting in continuation from the dorsolateral edges of the supraoccipital. The ventrolateral ends of the processes are expanded both dorsally and ventrally. The dorsal expansion is more abrupt and distinct than the ventral one, so that the paroccipital process, together with the posttemporal process of the supraoccipital–exoccipital–opisthotic complex encloses the ellipsoid posttemporal fenestra on three sides. The posterior side of the paroccipital process is dorsolaterally–ventromedially convex, and bears a ridge that originates at the dorsolateral corner of its base, and extends almost vertically to where the slight ventral extension of the outer end begins. This ridge is weakly rugose and might thus represent some muscle insertion. In ventral view, the edge of the paroccipital process expands anteroposteriorly and develops distinct ridges to enclose a fossa, which contains at least two deep foramina (probably for cranial nerves IX–XI; Janensch 1935; Upchurch *et al*. 2004a). The anteriormost crest extends onto the neighbouring bones of the braincase to form the crista prootica.

Basioccipital and basisphenoid. The basioccipital forms the main body of the occipital condyle. The sutures with the exoccipital are unclear but appear to extend obliquely so that the exoccipital contributes to only the laterodorsalmost corners of the occiput, as is the case in all known sauropods (Wilson & Sereno 1998; Upchurch *et al*. 2004a). The entire condyle has a straight dorsal margin, so that the outline becomes semicircular. Towards the foramen magnum, the neck of the occipital condyle develops a very slight midline concavity that leads into the endocranium. Two foramina are placed lateroventrally on the base of the neck of the occipital condyle, where also the paroccipital processes originate. These foramina are usually interpreted as the openings for cranial nerve XII (Janensch 1935; Upchurch *et al.* 2004a; Harris 2006a). The ventral face of the occipital neck curves gradually to form a deep and narrow U-shaped concavity between the basal tubera and the occipital condyle, when seen in lateral view.

Towards the paired basal tubera, the basisphenoid expands laterally so that the paired tubera equal about twice the width of the occipital condyle, which is considerably

more than in any other diplodocid and might thus represent an additional autapomorphy of *Kaatedocus siberi* (see Mannion 2011, table 1). From their ventrolateral corners, the basipterygoid processes extend anteroventrally for a short distance before curving outwards (forming an acute angle of about 26°) and finally exceed the width of the basal tubera. The tubera are only slightly distinct in ventral view, but appear as posteriorly projecting rugose knobs in lateral aspect. They are parallel to each other in ventral view, and separated by a narrow notch. Unlike in *Apatosaurus* YPM 1860, *Diplodocus hayi* HMNS 175 (= CM 662) and the flagellicaudatan braincase MB.R.2387, no foramen is present in this notch (Holland 1906; Remes 2009; pers. obs. 2011).

The bases of the slender basipterygoid processes are subtriangular and about a third to half of the width of their corresponding tuber. The processes become subcircular more distally, but maintain more or less the same width until they expand to a small degree transversely at their distal end. Although the mounted skull gives the impression that they would project directly ventrally, the disarticulated braincase and frontals clearly show that they actually were at an angle of about 45° to the skull roof. The basipterygoid processes are united at their bases by a thin bony sheet, originating at their ventral edges and extending anteroventrally to the point where the processes curve outwards. In anterodorsal view, this bony sheet bears the ventralmost point of the parasphenoid rostrum, which is broken off. From there, a thin but distinct ridge extends posterodorsally, until it reaches a small midline foramen around midlength of the entire braincase, posterior to the larger opening for the optic nerve. This ridge borders two large oval symmetrical fossae extending from the base of the basipterygoid processes to a point slightly anteroventral to the small foramen mentioned above. The fossae probably include the foramen for cranial nerve VI. They are symmetrical, and laterally bordered by the crista prootica that connects posterodorsally to the anterior side of the paroccipital processes.

Orbitosphenoid. The orbitosphenoids are paired bones that floor the braincase anteriorly and connect it with the frontals dorsally. The oblique posterolateral edges of the orbitosphenoids contact the laterosphenoids, but no clear suture is visible. In ventral view, the two orbitosphenoids form a transversely convex trapezoid structure with subparallel anterodorsal and posteroventral margins. The longer anterodorsal edge attaches to the frontals laterally and forms the ventral margin of the opening for cranial nerve I medially. At its midlength, a deep narrow notch is well marked, separating the two elements. The notch almost reaches the foramina for the cranial nerve II, which are medially conjoined and form a single opening, unlike *Apatosaurus* BYU 17096 (Balanoff *et al.* 2010) but similar to *Suuwassea* ANS 21122 (Harris 2006a; pers. obs. 2011).

Laterosphenoid. The laterosphenoids floor the braincase lateroventrally, being capped by the frontals and parietals dorsally, and contacting the orbitosphenoid and prootic anteromedially and posteromedially, respectively. At the posteriormost corner of the barely recognizable suture with the orbitosphenoid, slightly dorsally to posterodorsally of the foramen for the cranial nerve II, a smaller, ellipsoid fossa appears to bear two foramina for the cranial nerve III and IV. These foramen are usually thought to mark the suture between orbitosphenoid and laterosphenoid (Upchurch *et al.* 2004a), but are located more anteriorly in, for example, *Suuwassea emilieae* ANS 21122 (Harris 2006a). The lateral edge of the laterosphenoid bears a conspicuous lateroventrally projecting process that tapers towards its end, and that *in vivo* would probably have contacted the medial end of the ventral margin of the postorbital dorsomedial process. This process marks the origin of the crista antotica, which then extends ventrally along the lateral side of the braincase to merge with the crista prootica. The crista antotica thereby separates the more posteriorly situated foramen for cranial nerve V from the two anteroventrally placed foramina for cranial nerves III and IV.

Prootic. The two prootics floor the braincase lateroventrally and do not show any midline contact. They meet the basisphenoid ventrally, the laterosphenoid anteriorly, and at least the exoccipital–opisthotic complex dorsally, and are separated by the midline ridge originating at the parasphenoid rostrum, and the adjacent fossae for cranial nerve VI. Its sutures are difficult to observe, the only hints to them are the various foramina that have previously been interpreted to pierce the prootic at the base of the paroccipital process, towards the ventral midline of the braincase and anterodorsally (see above and Upchurch *et al*. 2004a; Carabajal *et al*. 2008). The prootic bears a major part of the crista prootica that originates at the base of the paroccipital processes and from there passes laterally on the prootic in the direction of the basal tubera, bordering the trigeminal foramen posterodorsally on its way. Further ventrally, it merges with the crista antotica and develops a thin bony shelf lateral to the basal tubera, distinct, but without a conspicuous lateral process as present in *Dicraeosaurus* (Janensch 1935; Upchurch *et al*. 2004a) or *Amargasaurus* (Salgado & Bonaparte, 1991; Upchurch *et al.* 2004a).

Mandible

Dentary. Both dentaries are only partially preserved, the right element lacking a median portion of the tooth-bearing dorsal edge, and the posteriormost part. The left element only preserves the anteroventral portions. The bones are labiolingually compressed, and slightly thicker dorsally than ventrally, where they taper to a sharp edge. In ventral view the dentaries gently curve medially at their anterior ends, similar to the juvenile *Diplodocus* CM 11255

(Whitlock *et al*. 2010), but in contrast to the squared shape of the lower jaw of *Diplodocus* CM 11161 (McIntosh & Berman 1975; Whitlock 2011a). In lateral view, the ventral margins of the dentaries develop a weak posteroventrally projecting process close to the symphysis, so that the entire border is slightly concave anteroposteriorly. This process does not form such a sharp 'chin' as described in *Diplodocus* or *Dicraeosaurus* (Janensch 1935; Upchurch 1998; Whitlock 2011a), but is still distinctive. The symphysis itself has a subrectangular outline, and is oriented obliquely in a way that its dorsal end projects further anteriorly than the ventral 'chin'. It marks also the highest part of the dentaries, which become gradually constricted dorsoventrally up to the posteriormost alveolus.

Although in both elements the total number of alveoli is not preserved, the position of the posteriormost alveolus in the right jaw and the accompanying grooves on the ventral portion indicate that 12 or 13 dentary teeth were present. They do not reach as far back as the maxillary teeth, so that a crown-to-crown occlusion does not appear to have occurred. Posteriorly, there is no indication of a prominent coronoid eminence, as is the case within all Diplodocoidea (Upchurch et al. 2004a). However, due to its incomplete preservation, an abrupt dorsal expansion for a shallow eminence similar to the one present in *Diplodocus* CM 11161 (McIntosh & Berman 1975) cannot be excluded.

Surangular. The probable right surangular is mistakenly mounted as a left angular. It is anteroposteriorly straight and contributes the posterior part of the dorsal edge of the lower jaw. This dorsal margin is mostly straight in lateral view, only at its posteriormost fifth of the entire length it first curves weakly laterally, before it turns to project ventrally and slightly medially, to cover the outer surface of the articular, and to initiate the medial bowing of the retroarticular process of the jaw. The ventral border is highly concave, with the most constricted part close to the point where the opposing edge bows ventrally. Slightly anterior to this point, there is a well-developed foramen at the anterodorsal end of a short oblique groove. Not far anterior to this foramen, accompanied by the dorsoventral expansion of the anterior portion of the surangular, a shallow dorsoventral concavity develops, which extends up to the anteriormost visible part.

Articular. Both articulars of SMA 0004 are preserved. They bear the articulation surface for the joint with the quadrate, and bow medially in respect to the long axis of one ramus of the lower jaw. The articular facet lies slightly below the level of the tooth row in lateral view. In addition to the concave facet for the articulation with the quadrate, also the medial and lateral sides bear shallow dorsoventral concavities. The lateral side is less high in this respect than the medial one, but reaches further posteriorly in lateral aspect, which is mostly due to the medial bowing of the posterior end of the bone. The posterior end has a subtriangular cross section, with a very narrow ventral surface and the two slightly inclined lateral and medial sides. This inclination gives room for the further needed mediolateral expansion towards its anterior end, where the articular facet is situated.

Cervical series

Proatlas. SMA 0004 only preserves the left proatlases, the mount at SMA includes a right element of a pair of proatlases (Figs 3–6) found approximately 7 m east of where the holotype of *Kaatedocus siberi* was found. The left element lacks its distal tip but is otherwise complete. To our knowledge, this is the first reported proatlas of any diplodocid sauropod. The proatlas consists of two symmetrical, wing-like bones with a relatively broad base and bluntly pointed, backwards, outwards and downwards pointing distal ends. The proatlas attaches to the exoccipital–opisthothic complex, just above the foramen magnum. The general shape of the proatlas in SMA 0004 is very similar to proatlaseses of *Dicraeosaurus*, *Giraffatitan* and *Camarasaurus* (Janensch 1929, 1950; Madsen *et al*. 1995). The base of the proatlantal elements is broader mediodorsally than lateroventrally, so that its cross section is ovoid. Whereas the outer surface remains shallowly convex, the inner side flattens after approximately one third of its entire length and even becomes slightly concave towards its distal end, where it caps the anteriormost part of the atlantal neural arch. In dorsal view, the entire bone is curved with its anterior and posterior edges being concave and convex, respectively.

Atlas–axis complex. The atlas–axis complex is complete, except for the ribs (Fig. 7). The general morphology is similar to that of *Apatosaurus louisae* CM 3018 and *Suuwassea emilieae* ANS 21122 (Gilmore 1936; Harris 2006b). The atlas anterior articulation tapers anteroventrally, forming the acute ventral 'lip' typical for flagellicaudatans (Fig. 7B; Mannion *et al.* 2012; Whitlock 2011a). In ventral view, the parapophyses project ventroposteriorly. Dorsal to this, small and shallow pneumatopores occupy the posterior half of the centrum. The centrum is fused to the atlantal neuroapophysis. These have a wing-like shape, with a long posterior and a very short anterior projection. The neurapophyses do not meet at the midline.

The axial centrum is long (more than three times its dorsoventral height), with a long, undivided pleurocoel occupying most of the lateral aspect. In ventral view the centrum is hourglass-shaped and flat. The anterior expansion is confluent with the parapophysis, while the posterior expansion has two small longitudinal ridges, which on more posterior vertebrae form the posteroventral flanges. The anterior condyle of the centrum has a midline dorsal projection that articulates with the atlas. The neural arch pedicels are short anteroposteriorly, occupying only half of the dorsal side of the centrum. This is in contrast to

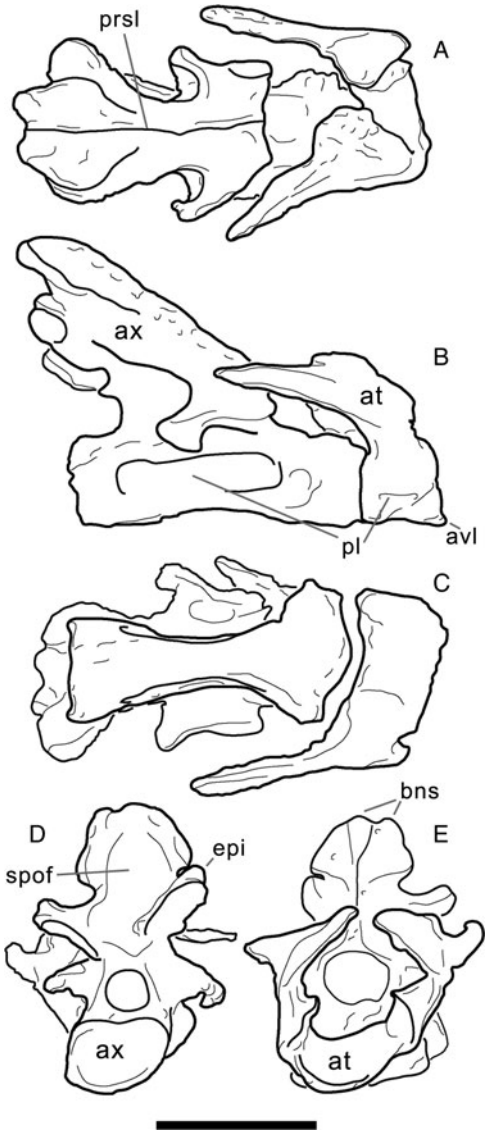

Figure 7. Drawings of the atlas–axis complex of the holotype of *Kaatedocus siberi* (SMA 0004; assignment of axis uncertain, see text) in **A,** dorsal, **B,** right lateral, **C,** ventral, **D,** posterior, and **E,** anterior views. Scale bar = 4 cm.

other diplodocids, such as *Apatosaurus louisae* CM 3018 or *Diplodocus carnegii* CM 84, where they cover almost the entire centrum (Hatcher 1901; Gilmore 1936). The posterodorsal and anterodorsal sections of the axial centrum of SMA 0004 are therefore free and not attached to the pedicels, unlike most diplodocids.

The axial neural arch is tall (more than 2.5 times the height of the centrum). The neural spine summit has a paired projection giving a bifid aspect. Anteriorly, there is a midline prespinal lamina that is straight in lateral view. The neural spine is inclined posterodorsally at an angle of 45°. Posteroventrally, the spinopostzygapophyseal laminae enclose a deep spof. Small epipophyses and pre-epipophyses are present. The diapophyses are mound-like posterolateral projections situated at the base of the neural arch and in the middle of the vertebra in lateral view.

Anterior cervical vertebrae (CV 3-5). The anterior cervical vertebrae are complete and only slightly deformed (Fig. 8; Table 1). The cervical ribs are fused to the vertebrae, only marked by a rugose and slightly expanded area. The neurocentral suture is closed and not discernable. The vertebrae are longer than high, with the cervical ribs not projecting far beneath the ventralmost point of the centrum. The opisthocoelous centra have EI values between 3.1 and 3.6 (Table 2). The posterior extremities are higher than wide, and broader dorsally than ventrally, forming a subtrapezoidal outline. Whereas the hemispherical anterior condyle is continuous with the centrum in CV 3, it is separated from the rest of the centrum by a shallow ridge in CV 4 and 5. Its surface is slightly more irregular compared to the other portions. The condyle of CV 5 shows two distinct invaginations dorsomedially (Fig. 8, B5). As there is no other element that bears such a structure on its condyle, a taphonomic cause is probable, although the more dorsally located indentation lies more or less on the midline and resembles a foramen. However, a connection with the internal structures cannot be identified with certainty.

The lateral sides of the centra of CV 3 to 5 are straight dorsally but have a somewhat sinuous outline ventrally. The ventral edge extends ventrally from the anterior condyle backwards to where the parapophysis is situated. At the posterior end of the parapophysis, it becomes strongly concave, with the most constricted point slightly anterior to the centrum midlength. The posterior portion is again expanded ventrally but curves back dorsally to a very small degree just before reaching the posteroventral corner. The median constriction is more pronounced the more posterior the element is in the cervical column. The lateral surfaces of the centra bear a large pleurocoel, which is undivided in CV 3 and 4 but separated into two by a median ridge in CV 5. The pleurocoels are bordered medially by a very thin wall and occupy almost the entire length of the vertebral centra. Whereas the anterior border of the coels in CV 3 and 4 is clearly defined, the posterior end is created by the gradual curvature of the cotyle. Following the overall aspect of the lateral surface of the centra, the pleurocoels expand dorsoventrally posteriorly. In CV 5, an oblique, shallow ridge divides the pleurocoel into a shorter anterior and a longer posterior pneumatic fossa (Fig. 8, B2). The anterior depression has a very distinct and continuously rounded anterior edge, while its posterior end is more pointed due to the anterodorsally–posteroventrally extending ridge that divides the pleurocoel. This ridge reaches the ventral margin of the centrum at its most dorsoventrally constricted point and is more or less continuous with the posterior part of this concave portion of the ventral edge. The posterior pneumatic fossa of CV 5 has thus a subtriangular outline, with

Table 1. Measurements of CV 3–14 of the holotype of *Kaatedocus siberi* (SMA 0004).

	Measurements (mm)														
	gl	gh	cl	cmw	wd	wpr	wpo	ppl	pph	wct	hct	wcd	hcd	hns	cl-wo-cd
CV 3	134	89	113	8	43	49	44	90	18	28	36	19	23	48	110
CV 4	151	92	131	11	57	43	51	103	20	36	39	20	27	59	118
CV 5	206	97	165	14	63	58	51	129	27	42	46	29	35	59	135
CV 6	227	108	194	14	69	49	64	134	22	49	47	37	38	65	184
CV 7	268	134	227	17	82	71	62	151	25	40	62	48	43	80	203
CV 8	297	138	245	23	105	77	79	161	39	49	74	49	49	91	213.5
CV 9	309	161	270	39	109	80	82	168	28	40	77	50	54	106	231
CV 10	338	183	273	40	126	94	92	176	30	60	91	62	63	120	241
CV 11	324	202	298	50	125	74	92	172	37	78	100	68	84	124	253
CV 12	327	221	314	60	138	108	108	169	35	85	102	71	95	147	264
CV 13	309	250	322	67	182	116	98	182	28	84	125	76	102	172	269
CV 14	302	273	312	68	203	113	112	155	28	84	118	70	110	182	244

	Ratios													
	wd/gh	wd/gl	gh/cl	cl/ wct	hct/ wct	cl-wo-cd/hct	cl/hct	hns/hct	ppl/cl	gl/cl	hns/gl	wd/wct	hns/wd	hns/gh	gh/gl
CV 3	0.48	0.32	0.79	4.04	1.29	3.06	3.14	1.33	0.80	1.19	0.36	1.54	1.12	0.54	0.66
CV 4	0.62	0.38	0.70	3.64	1.08	3.03	3.36	1.51	0.79	1.15	0.39	1.58	1.04	0.64	0.61
CV 5	0.65	0.31	0.59	3.93	1.10	2.93	3.59	1.28	0.78	1.25	0.29	1.50	0.94	0.61	0.47
CV 6	0.64	0.30	0.56	3.96	0.96	3.91	4.13	1.38	0.69	1.17	0.29	1.41	0.94	0.60	0.48
CV 7	0.61	0.31	0.59	5.68	1.55	3.27	3.66	1.29	0.67	1.18	0.30	2.05	0.98	0.60	0.50
CV 8	0.76	0.35	0.56	5.00	1.51	2.89	3.31	1.23	0.66	1.21	0.31	2.14	0.87	0.66	0.46
CV 9	0.68	0.35	0.60	6.75	1.93	3.00	3.51	1.38	0.62	1.14	0.34	2.73	0.97	0.66	0.52
CV 10	0.69	0.37	0.67	4.55	1.52	2.65	3.00	1.32	0.64	1.24	0.36	2.10	0.95	0.66	0.54
CV 11	0.62	0.39	0.68	3.82	1.28	2.53	2.98	1.24	0.58	1.09	0.38	1.60	0.99	0.61	0.62
CV 12	0.62	0.42	0.70	3.69	1.20	2.59	3.08	1.44	0.54	1.04	0.45	1.62	1.07	0.67	0.68
CV 13	0.73	0.59	0.78	3.83	1.49	2.15	2.58	1.38	0.57	0.96	0.56	2.17	0.95	0.69	0.81
CV 14	0.74	0.67	0.88	3.71	1.40	2.07	2.64	1.54	0.50	0.97	0.60	2.42	0.90	0.67	0.90

Note: gl (greatest length); gh (greatest height); cl (centrum length); cmw (centrum minimum width); wd (width across diapophyses); wpr (width across prezygapophyses); wpo (width across postzygapophyses); ppl (pneumatopore length); pph (pneumatopore height); wct (width posterior cotyle); hct (height posterior cotyle); wcd (width anterior condyle); hcd (height anterior condyle); hns (height neural spine); cl-wo-cd (centrum length without condyle).

its hypotenuse being formed by the separating ridge and the ventral margin of the lateral surface. The horizontal dorsal margin is more distinct than the ventral margin.

The ventral side of the centra of CV 3 to 5 is marked by a strong constriction slightly anterior to midlength and posterior to the parapophyses, so that the centrum has an irregular hourglass-shaped outline in ventral aspect, which is most pronounced in CV 4. Whereas the parapophyses are attached to the anterior condyle in CV 3, they become detached in the subsequent vertebrae. In all three elements, the parapophyses project ventrolaterally and are longer than wide. Together with the posterior end of the condyle they enclose a shallow subtriangular concavity. The dorsal surfaces of the parapophyses of CV 5 are concave, so that the pneumatic fossa appears to be extended onto the parapophysis. An indistinct ridge separates the fossa into two smaller depressions. The transverse constriction of the ventral sides occupies mainly the anterior second fourth of the surface, and is flat to slightly convex in CV 3 and 4, but concave in CV 5. Posterior to the constriction, the lateral edges develop ventrally to lateroventrally projecting, thin flanges that border a second, larger cavity. These flanges become oriented subparallel in the last fourth of the ventral surface, and gradually disappear shortly before they reach

Table 2. Elongation indices of the CV of the holotype of *Kaatedocus siberi* (SMA 0004).

	EI	mean EI
CV 3	3.14	
CV 4	3.36	3.36
CV 5	3.59	
CV 6	4.13	
CV 7	3.66	
CV 8	3.31	3.52
CV 9	3.51	
CV 10	3.00	
CV 11	2.98	
CV 12	3.08	2.88
CV 13	2.58	
CV 14	2.64	

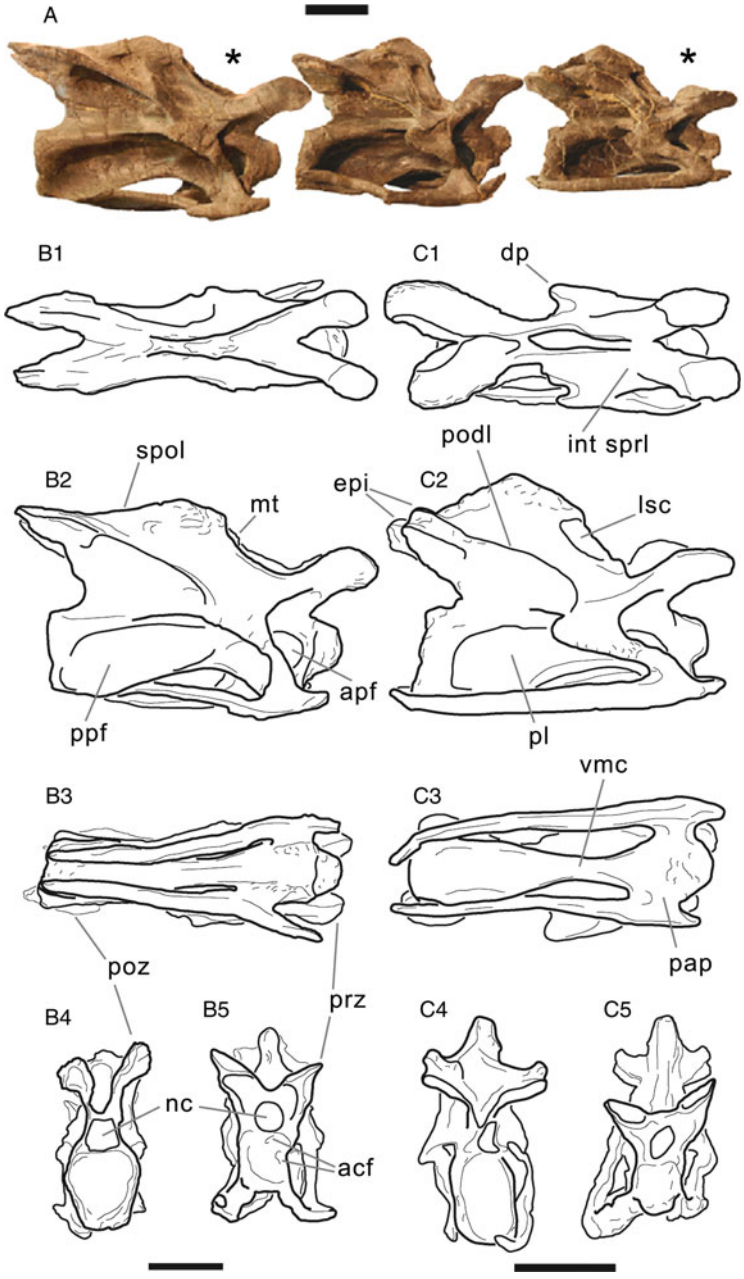

Figure 8. A, Photograph and **B, C,** drawings of the anterior cervical vertebrae of the holotype of *Kaatedocus siberi* (SMA 0004). Photographs in lateral view and to scale, elements shown in the drawings are indicated by an asterisk. Drawings of CV 5 (B), and CV 3 (C) in dorsal (1), lateral (2), ventral (3), posterior (4) and anterior (5) views; scaled to the same centrum length, in order to highlight changes of proportions. Scale bars = 4 cm.

the posterior edge of the centrum. In posterior view, they almost reach the ventral level of the cervical rib shafts.

The neural arches of CV 3 to 5 exceed both the length and the height of the centra by two to four centimetres. The spine summit is elevated above the postzygapophyses in CV 3 and 4 but is at about the same height in CV 5. It is slightly anteriorly inclined in CV 4 and 5. With the exception of CV 3, where the prezygapophyses mark the widest point of the vertebra, all cervical vertebrae are widest across their diapophyses. The outline of the prezygapophyseal facets is highly variable, being subrectangular in CV 3 (with the longer diameter extending anteroposteriorly), subtriangular in CV 4 (with the anterior end pointed and the posterior edge straight), and rather rounded in CV 5. The facets are well separated from the prezygapophyseal process in CV 3 but less so in the subsequent elements. As in all

Diplodocinae that preserve cervical vertebrae, the prezygapophyseal facet surfaces are somewhat convex both anteroposteriorly and transversely (e.g. Hatcher 1901; McIntosh 2005). In anterior view they face inwards and upwards, at an angle of about 45° to the horizontal. The prezygapophyses are supported by a stout single centroprezygapophyseal lamina extending anteriorly as well as dorsally and laterally until it curves to project almost straight anteriorly. The cprl unites with the anterior end of the prdl ventral to the posteriormost point of the articular facet in CV 3. This cannot be observed in CV 4 and 5, because the prdl disappears towards its anterior end. The course of the prdl cannot be followed further than to a point lateroventral to the posteriormost extension of the articular facets. The tprl develops approximately at midlength of and ventral to the articular facets, and extends backwards to the base of the process where the two portions of the right and the left side unite in a very acute angle. Together with the cprl and the neural canal roof, the tprl forms two small centroprezygapophseal fossae (cprf).

The sprl originates on the posterolateral corner of the prezygapophyseal facet but disappears shortly posteriorly. Its course is difficult to follow in CV 3 and 4. In CV 3 a median, slightly bifid crest originates posterior to where the right and left parts of the tprl unite. It is posteriorly inclined at about 50° to the base of the neural canal. At midlength, the bifurcation becomes suddenly somewhat deeper and the inclination of the sprl decreases to approximately 40° while proceeding to the spine summit. In CV 4 a trifid median crest develops behind the union of the tprl. It is slightly inclined posteriorly in its ventral portion, which is longer than the corresponding structure of CV 3. The median ridge on the trifid crest disappears dorsally, where the lateral edges become suddenly more developed, and even project anteriorly to a small degree, before they extend straight posterodorsally to reach the spine summit. The sprl of CV 5 are the easiest to observe. At the base of the spine, they turn to proceed dorsally at an angle of 25–30° towards the spine summit. Shortly before the sprl meet at the dorsalmost point of the neural spine, a median bony structure appears and projects somewhat anteriorly (Fig. 8, B2). From this point the sprl bend and proceed straight dorsally before turning backwards to reach the uppermost point of the vertebra. In all three anterior cervical vertebrae the two sprl meet the spol at the spine summit where they are interconnected such that the spine cannot be interpreted as being entirely bifid. This contrasts with the state in *Diplodocus* and dicraeosaurids where the bifurcation of the cervical vertebrae also affects the anteriormost elements (e.g. Hatcher 1901; Janensch 1929).

The spine summit is transversely compressed and forms a blunt apex in lateral view. It is located posterior to the posteriormost point of the diapophysis. The lateral side of the neural spine bears a distinct, dorsoventrally elongated fossa posteriorly adjacent to the sprl. Additional, shallower cavities are present in CV 4 and 5, ventral and posterior to the distinct fossa, respectively. The diapophysis is situated on the anterior second quarter of the vertebral centrum. It is defined by the prdl anteriorly, the podl posterodorsally, the nearly horizontal pcdl posteriorly, and a very short acdl anteroventrally. The pcdl is relatively short compared to its length in more posterior elements and disappears considerably anterior to the posteriormost extension of the pleurocoels. In lateral view the diapophysis of CV 3 describes a strong backwards curve due to a rounded posterior projection and the strongly anteroventrally protruding articular end. Whereas the latter remains similar in the following vertebrae, the posterior edge of the diapophyses of CV 4 and 5 bear subsequently less-developed posterior projections. The podl of CV 3 to 5 is gently curved. It originates at an acute angle with the diapophysis (approximately 55° to the horizontal), and becomes almost horizontal at the postzygapophyses.

The postzygapophyses are inclined posteriorly and bear large and suboval facets, with their longest diameter oriented anteroposteriorly. The facets face downwards and somewhat outwards and backwards. They are concave mediolaterally, and extend anteriorly to a point almost straight above the posteriormost point of the pedicels of the neural arch. In posterior view, the tpol continues the curvature of the facets until the two sides unite, where they meet the roof of the neural canal. Dorsally, the postzygapophyseal facets are capped by very distinct epipophyses that overhang the facets both laterally and posteriorly. Their lateral margins are confluent with the podl. While the posterior edge of the epipophysis is rounded in CV 3, it becomes more and more pointed in the subsequent elements. Such a strong development of the epipophyses is rarely seen in other diplodocids. Whereas epipophyses are present in most taxa, they usually do not form a pointed posterior end that overhangs the articular facet (e.g. AMNH 6341; CM 84, 94, 11984; DNMS 492, 1494; Hatcher 1901; McIntosh 2005; pers. obs. 2011). In CV 5 the spol and the podl unite at the very acute posterior end of the epipophysis. The spol extends straight and includes an acute angle of approximately 40° with the podl in lateral view in CV 3. In the more posterior elements this angle decreases to about 35° in CV 4 and 30° in CV 5.

Mid-cervical vertebrae (CV 6-10). Some of the mid-cervical vertebrae show minor compression, caused by shearing (CV 7, 8) or weak crushing (CV 10), but are preserved complete. They are well fused with the neural arches and the cervical ribs. The vertebrae are longer than high, and higher than wide (Table 1). The opisthocoelous centra are axially long and somewhat higher than wide at their posterior end. With a mean EI of 3.5, the mid-cervical vertebrae constitute the most elongated centra of the series, which lies between the values reported for *Apatosaurus* or *Diplodocus* and *Barosaurus* (McIntosh 1990, 2005; Wedel

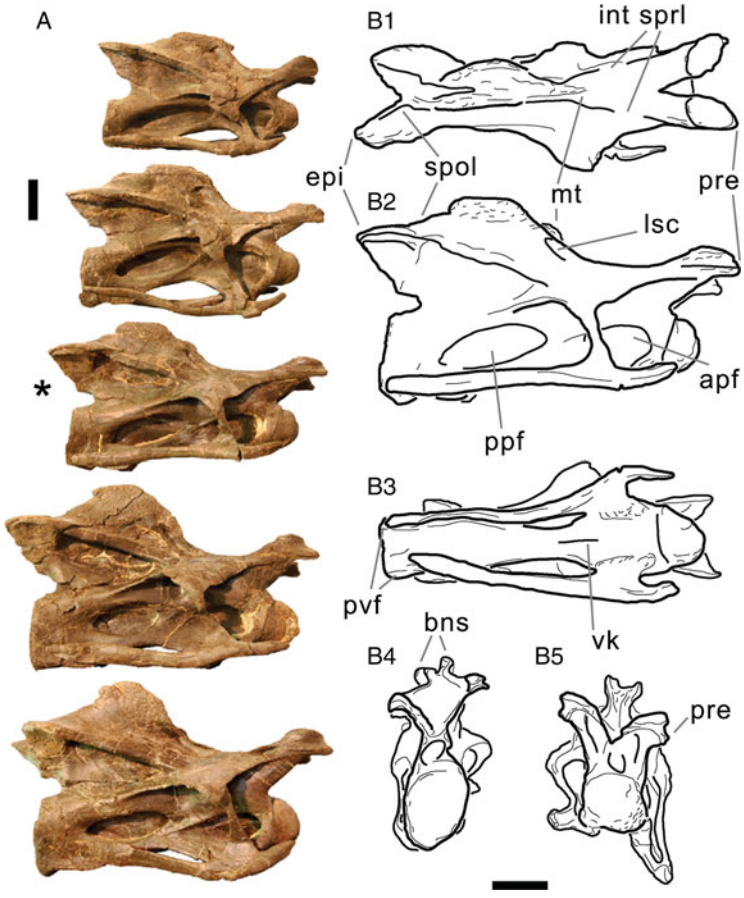

Figure 9. A, Photograph and **B,** drawings of the mid-cervical vertebrae of the holotype of *Kaatedocus siberi* (SMA 0004). Photograph in lateral view and to scale, CV 8 shown in the drawings is indicated by an asterisk. Drawings of CV 8 (B) in dorsal (1), lateral (2), ventral (3), posterior (4) and anterior (5) views. Scale bars = 4 cm.

et al. 2000). CV 6 is the most elongated element of the cervical column (Table 2).

In CV 7 to 10 the well-developed, hemispherical anterior condyle is separated from the rest of the centrum by a weak but easily discernible ridge extending anterodorsally–posteroventrally (CV 7 to 9), or subvertically (CV 10) on its lateral sides, and straight transversely dorsally and ventrally. Whereas in CV 6 to 9 the outline of the condyle is subcircular in anterior view, in CV 10 it is broader dorsally than ventrally. The surface of the articular ball and around its posterior ridge is irregular. The subdivision of the pleurocoel becomes subsequently more distinct from anterior to posterior, with even a weak subdivision of the anterior coel in CV 10. Here, faint ridges are located at about midheight both anteriorly and posteriorly. Between the two pleurocoels, a relatively wide bony shelf develops in CV 8 (Fig. 9, B2) and more posterior elements, bearing an oblique, anteriorly inclined ridge extending from the posterodorsal corner of the anterior pneumatic fossa downwards and backwards, before it diminishes in about the middle of the bony shelf. The anterior pneumatic fossa of CV 8 to 10 shows a very gradual transition onto the bony shelf between the two depressions. Whereas in all mid-cervical vertebrae the pneumatic fossae are completely separated ventrally, a combined dorsal margin can still be seen in CV 6 and 7. The posterior fossa becomes more restricted posteriorly in more posterior elements, so that both the anterior and posterior portion together occupy less and less of the entire centrum length. The shape of their outlines remains practically the same in all mid-cervical vertebrae: the anterior coel is subcircular and relatively short, while the posterior coel is more lens-shaped with pointed ends anterodorsally and posteroventrally. In CV 8 the upper edge of the posterior pleurocoel is more curved than the lower margin (Fig. 9, B2).

In ventral view the vertebral centrum is broadest anteriorly where the parapophyses are situated. The transverse constriction of the mid-cervical centra migrates more posteriorly than the more anterior elements, so that it now marks the middle third. Whereas in CV 6 this portion is slightly transversely convex, it is flat to shallowly concave in more posterior vertebrae. The depression between the

parapophyses is interrupted medially by a shallow ridge. This is only visible between the posterior end of the parapophyses and the narrowest point of the centrum but becomes more pronounced in the more posterior elements of the cervical series. The parapophyses point lateroventrally and are longer than wide. They are located beneath the anterior pneumatic fossa in lateral view, which extends slightly onto the dorsal surface of the parapophyses. At the base of the parapophysis a shallow ridge divides this extended coel into a dorsal portion (lying on the centrum) and a ventral part lying on the parapophysis.

The neural arch of CV 6 to 8 is dorsoventrally shorter relative to centrum length compared to the anterior cervical vertebrae and the more posterior elements. In all mid-cervical vertebrae it exceeds the centrum in length anteriorly but only very little posteriorly. The prezygapophyses project anteriorly, dorsally, and slightly laterally, beyond the anterior condyle. The articular facets are anteroposteriorly elongated and well offset from the rest of the prezygapophysis. The facets are transversely as well as anteroposteriorly convex and are supported ventrally by the cprl. Like the anterior cervical vertebrae the prezygapophyses of CV 6 are laterally flat and smooth. On the other hand, CV 7 to 10 exhibit an initially shallow, but in more posterior elements, pronounced horizontal ridge that extends ventral and parallel to the articular facet, connecting the sprl with the prdl. Together they form a distinct anteriorly projecting spur that extends considerably beyond the anterior edge of the prezygapophyseal articular facet. A similar ridge and spur is also present in the holotype of *Australodocus bohetii* (MB.R.2455; Remes 2007; pers. obs. 2011) and appears homologous to the pre-epipophysis described in *Euhelopus* and other titanosauriforms (Wilson & Upchurch 2009; Whitlock 2011c). Whereas the ridge is also present in a number of diplodocids (e.g. *Apatosaurus* sp. AMNH 550; *Diplodocus carnegii* CM 84; *Barosaurus* sp. CM 11984; pers. obs. 2011), it does not project beyond the anterior margin of the facets in these taxa. The spur can thus be considered a local autapomorphy of *Kaatedocus siberi*.

Posteroventral to the pre-epipophyseal ridge in CV 9 and 10 a distinct cavity marks the anteriormost extension of the sdf, which is relatively shallow. The cavity is bordered dorsally by the posteriormost extension of the pre-epipophysis and by the here laterally inclined anteriormost portion of the sprl. In CV 10 a second, indistinct crest developed subparallel to and between the facet and the pre-epipophysis. The anterior spur in CV 7 to 10 is ventrally confluent with the cprl as well, which borders the deep cprf. The tprl of all mid-cervical vertebrae form a V-shape in dorsal view, and meet the roof of the neural canal at their posteriormost extension.

The sprl becomes reduced to a shallow ridge towards the base of the prezygapophysis, before it curves dorsally again (Fig. 9, B1). Anteriorly, it connects to the posterolateral corner of the articular facet, as in the anterior cervical vertebrae. The curvature of the sprl in lateral view becomes more pronounced in the more posterior elements. The sudden posterior bend that marked the sprl of the previous cervical vertebrae also occurs in CV 6 and 7 but even closer to the level of the neural spine top, so that the lamina extends almost horizontally towards the dorsalmost point of the spine. In CV 8 and 9 this last portion of the sprl is oriented straight horizontally, and thus forms the spine summit, whereas in CV 10 the sprl develops another backwards bend anteroventral to the summit. The lateral cavity of CV 6 and 7 is situated more dorsally than in the anterior cervical vertebrae but remains restricted to the lower half of the sdf in CV 8 to 10. It is much more distinct than in *Diplodocus carnegii* CM 84, and more ventrally located compared to *Barosaurus* sp. CM 11984 (Hatcher 1901; McIntosh 2005; pers. obs. 2011). Anterior and medial to the sprl, the median ridge is more developed than in any previous elements, and bears a distinct anterior projection in CV 6 and 7. The ridge connects posteriorly with the now anteroposteriorly elongated area, where both sprl and spol unite to create a single neural spine summit. In CV 8 to 10, the anterior projection becomes lost, and the sprl and spol begin to develop dorsal projections that exceed the median ridge laterally, so that CV 8 and more posterior elements are the first to exhibit more and more bifurcated neural spines. This configuration shows that the median ridge probably represents the true neural spine, and is equivalent to the structure termed by Schwarz *et al.* (2007a) the median tuberosity, a flagellicaudatan synapomorphy (Mannion *et al.* 2012; Whitlock 2011a). As with the lateral cavity within the sdf, the median tuberosity becomes reduced again in CV 8 to 10, and both structures remain restricted to about the same height.

The mid-cervical spine summit is rugose laterally and posteriorly offset from the rest of the spol. In anterior view, the transversely narrow metapophyses are subparallel to slightly laterally inclined. In dorsal view the metapophyses of CV 8 to 10 have a very transversely compressed but subtriangular cross section, with a flat outer surface and an angled medial side. From this medialmost point a step-like structure extends anteroventrally and connects the top with the posterior corner of the true neural spine. The summit sits above the central third of the centrum length in CV 6 and 7, above the posterior second fifth in CV 8 and 9, and slightly more anteriorly in CV 10.

The diapophysis overlaps the anterior second quarter of the centrum. It is formed by the prdl anteriorly, the podl posterodorsally, the pcdl posteriorly, and a short acdl anteroventrally. The podl is anteroposteriorly concave in dorsal view. In lateral aspect it is gently curved in CV 6 and 7 but straight in CV 8 to 10. The angle that the podl forms with the base of the neural canal decreases from approximately 25° in CV 6, to 20° in CV 7 to 9, and finally to about 18° in CV 10. In the latter the podl is supported by a small accessory lamina immediately after it originates

on the base of the diapophysis. This accessory lamina is well visible in posterolateral view, and its free edge faces posteriorly. The acdl separates the well-developed prcdf and the cdf. It extends upwards and backwards in its anterior portion, but curves to become almost vertical below the diapophysis. With the exception of CV 9 and the right side of CV 8, the posterior edge of the mid-cervical diapophyses develops a very short posterior projection similar to but much less pronounced than in CV 3 and 4. The articulation with the tuberculum in the mid-cervical vertebrae is weakly posterodorsally inclined.

The postzygapophyses are transversely deeply concave in posterior view. Whereas the postzygapophyses of CV 6 have rounded posterior edges in dorsal view, they are more pointed in CV 7 to 10. The articular facets are subtriangular, and wider than long. Their anterior edges mark the posterior extent of the postzygapophyseal centrodiapophyseal fossa. The tpol unite medially straight above the posterior edge of the centrum, and not slightly inset as in the previous vertebrae. In lateral aspect the neural arch thus describes a regular U-shape in its posteroventral corner, before it bends dorsally to follow the posterior margin of the postzygapophyseal articular facets. The epipophyses are less developed than in the anterior cervical vertebrae, but still overhang the articular facets both laterally and posteriorly. As in the anterior cervical vertebrae, both spol and podl insert in the epipophysis. The spol is straight in CV 6 and 10, but slightly convex in CV 7 to 9 (most so in the left spol of CV 7, where it forms a step-like configuration).

Posterior cervical vertebrae (CV 11-14). The posterior cervical vertebrae (Fig. 10) are complete and well preserved, although the bone surface is mildly crushed and slightly deformed in most elements. The vertebrae and cervical ribs are well-fused and the transition is rugose but not well marked by a line. The vertebrae as a whole are longer than high, and higher than wide, exhibiting increasing ratios towards a more posterior position in the cervical column (Table 1). The centra are strongly opisthocoelous and slightly higher than wide in posterior view. The EI of the posterior cervical vertebrae is approximately 3 in CV 11 and 12, decreasing to 2.6 in CV 13 and 14 (Table 2). The anterior condyle is very pronounced, hemispherical, and bordered by a ridge that is slightly anteriorly inclined (in CV 11 to 13) to almost vertical (in CV 14; Fig. 10, B2), and conspicuous in lateral and dorsal views but absent ventrally. The bone surface of the articular condyle is more rugose than the centrum.

Laterally, the centra of the posterior cervical vertebrae bear progressively more complex arrangements of laminae, ridges and depressions. In CV 11 two large pneumatic fossae form the main structure (Fig. 10, C2), together occupying about 60% of the lateral side. The anterior pneumatic fossa possesses two interior laminae that extend horizontally, the dorsal lamina being longer and more prominent. The anterodorsal rim of the pneumatic fossa is deep and well defined, while the posteroventral part becomes shallower and grades into the ventrolateral wall of the centrum and the parapophysis. The upper part of the pneumatic fossa is axially longer than the ventral part and is pointed posteriorly. The posterior pneumatic fossa is approximately 1.5 times longer than the anterior, and has a lens-like shape. The posterior and anterior ends form an acute angle and the entire pneumatic fossa is deep and well invaginated. The two pneumatic fossae are separated by a 3 cm wide longitudinal shelf that progresses diagonally in an anterodorsal–posteroventral direction and is reinforced by a ridge.

The anterior pneumatic fossa of CV 12 is highly similar to its corresponding structure in CV 11. It has tall margins anteriorly and dorsally, but grades onto a bony shelf posteroventrally. It is extended ventrally to also occupy the dorsal surface of the parapophysis, and subdivided into three areas by two unequally developed horizontal ridges. The posterior pneumatic fossa of CV 12, on the other hand, is different from the previous one. Two depressions are well separated from each other, but still united dorsally, where an anteroposteriorly long margin extends from the anterodorsalmost point of the posterior pneumatic fossa backwards and slightly downwards until it disappears at about mid-height on the centrum, below the posteriormost point of the pedicels. The anterior half of this crest roofs a very distinct, subtriangular (on the right side) to rhomboidal (on the left) depression. This depression is situated almost entirely beneath the pcdl, and bordered anteroventrally by the oblique bony shelf that also in the previous cervical vertebrae divides the anterior from the posterior coel. Ventrally, a broad ridge separates the larger anterodorsal subdivision of the posterior pneumatic fossa from a small oval depression posteroventral to it.

The lateral surfaces of CV 13 are marked by two deep pneumatic fossae anteriorly and posteriorly, which are subdivisions of more extended depressions that include smaller cavities as well. The general arrangement of these divided coels resembles the state in CV 12, except that the two most dorsal fossae are the most distinct and more anteroposteriorly elongated than in the previous element. Contrary to the state in CV 12, the more posterior of the two coels in CV 13 extends backwards beyond the posteriormost point of the pcdl. The small fossa that was clearly visible posteroventral to the subtriangular larger part of the posterior pneumatic fossa of CV 12 is reduced to a shallow concavity, of which the margins are unclear in CV 13. The portion of the centrum length that is occupied by the entire pleurocoelous structure decreases more or less continuously within the cervical column from 80% in CV 3 to 57% in CV 13.

In CV 14, two deeply invaginated pneumatic fossae represent the most distinct structures of the lateral surface

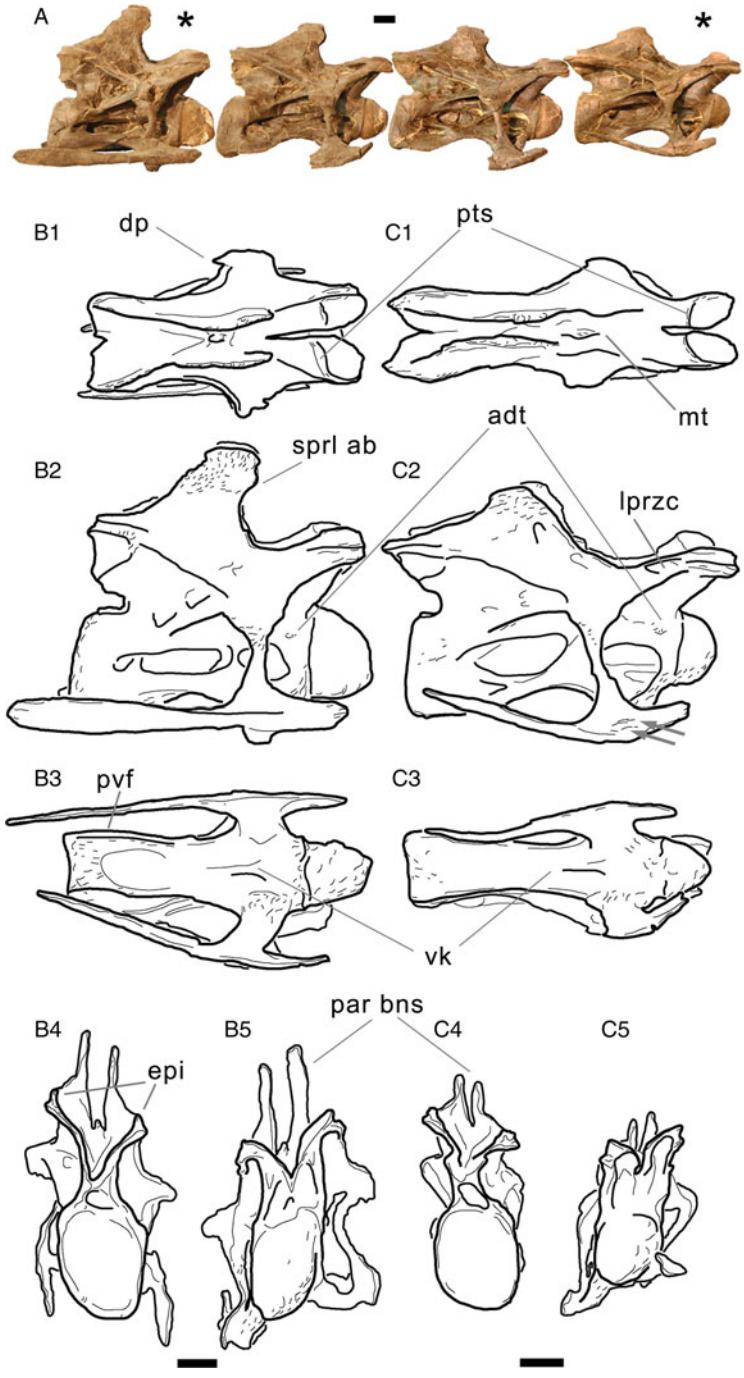

Figure 10. A, Photographs and **B, C,** drawings of the posterior CV of the holotype of *Kaatedocus siberi* (SMA 0004). Photographs in lateral view and to scale, elements shown in the drawings indicated by an asterisk. Drawings of CV 14 (B), and CV 11 (C) in dorsal (1), lateral (2), ventral (3), posterior (4) and anterior (5) views; scaled to the same centrum length, in order to highlight changes of proportions. Arrows in C2 mark possible bite marks. Scale bars = 4 cm.

(Fig. 10, B2). They are located anteriorly and posteriorly at the same level around mid-height on the centrum. Whereas both pneumatic fossae are of approximately the same dorsoventral height, the anterior coel is shorter anteroposteriorly by a third relative to the posterior one. It is of rhomboidal shape and subdivided into smaller cavities by three ridges: an oblique, anteriorly inclined crest that separates the posterodorsal corner; a horizontal ridge that extends from the posteroventral end of the previous ridge anteriorly; and a shallow ridge originating at the same point but proceeding anteroventrally. As in the preceding vertebrae with subdivided pleurocoels, the two major pneumatic

fossae of CV 14 are separated from each other by a ventrally oriented bony shelf. The latter bears a crest that originates at the posterodorsal corner of the anterior pneumatic fossa, and then proceeds ventrally before curving backwards to reach the posteroventral corner of the bony shelf. Here the ridge unites with the ventral edge of the posterior pneumatic fossa, which is anteroposteriorly elongated and slightly taller at the front than at the back. The dorsal edge of the posterior pneumatic fossa is straight and develops an almost horizontal bony strut at about midlength, which then proceeds anteriorly. Posteriorly, the dorsal rim exceeds the main coel to border a smaller depression behind the posterior pneumatic fossa, as in CV 12 and 13. This smaller cavity is subtriangular in CV 14, with an acute posterior end, and an almost vertical anterior rim that separates it from the main posterior pneumatic fossa. In the middle of the latter coel, a narrow horizontal crest is visible that does not connect to other morphological landmarks. It might thus also represent taphonomic deformation as the median wall separating the pleurocoels of the two sides at the centrum midline is extremely thin.

In all posterior cervical vertebrae, a rugose tuberosity is situated at the anterodorsal corner of the lateral side of the centrum (Fig. 10, B2 and C2). This tuberosity would be in line with a straight, imaginary extension of the anterior portion of the acdl. In CV 12 and 13 a weak striation connects these two structures. The only taxon that shows a similar feature is the probable dicraeosaurid *Suuwassea emilieae* (ANS 21122, pers. obs. 2011), but only in mid-cervical vertebrae (posterior cervicals are unknown in this taxon; Harris 2006b). The anterodorsal tuberosity can thus be considered at least a local autapomorphy (within Diplodocidae) of *Kaatedocus siberi*.

In ventral view the centrum of the posterior cervical vertebrae of SMA 0004 is hourglass shaped with a medium transverse constriction, which becomes less pronounced in more posterior elements. The surface is marked by two deep concavities, an anterior one bordered by the condyle and the two parapophyses, and a posterior one enclosed by the cotyle and two posteroventral flanges. The anterior concavity is subdivided by a midline ridge, which is located in the second quarter of the centrum length, and disappears at or somewhat anteriorly to the most constricted portion of the ventral surface. It is more distinct in more posterior vertebrae. The pair of flanges projects ventrally from each lateral side of the posteroventral corner of the centrum, but does not extend to the ventralmost rim of the cotyle. The flanges seem to clasp the distal end of the cervical ribs in some elements, but to what degree this is caused by taphonomic deformation is difficult to discern. If this represents the actual morphology it would probably be another autapomorphy of the new taxon. The parapophyses are at least twice as long as they are dorsoventrally high. They are positioned below the anterior pneumatic fossa in the first half of the centrum, and project to a small degree ventrolaterally.

The neural arch undergoes considerable changes throughout the posterior cervical vertebral series. It becomes both anteroposteriorly shortened, as well as dorsally elongated, and wider across the diapophyses towards more posterior positions. Whereas in CV 11 and 12 the neural arch still slightly surpasses the anterior or posterior rims of the centrum, CV 13 and 14 have subequally long arches and centra. The neural arch height/greatest length ratio remains around 30–40% in CV 3 to 11, but increases to 45% in CV 12, 56% in CV 13, and 60% in the last preserved vertebra. A similar increase can be observed in the width across diapophyses/greatest length ratio: this steadily rises from 30% in CV 6 to 39% in CV 11 and 42% in CV 12, after which it rises significantly to 59% in CV 13 and 67% in CV 14. In lateral view, also the orientation of the bifurcated neural spine changes within the posterior cervical vertebrae. In CV 11 (as also in the mid-cervical elements), the anterior corner of the spine summit marks the posteriormost extension of the sprl (Fig. 10, C2). In CV 12, the summit is located more anteriorly, arriving vertically above the posteriormost point of the now considerably curved sprl. This trend continues in CV 13 and 14, where the spine tops become even anteriorly inclined.

The prezygapophyseal facets are oblong to subtriangular, straight laterally and tapering somewhat medioposteriorly. They face dorsomedially and are slightly convex transversely. In anterior view the facets thus form a V. The distance between the two prezygapophyses is shorter than the width of a single zygapophysis, but this might be due to transverse taphonomic compression. The posterior rim of the articular facet is well marked and bordered by a ridge followed by a transverse sulcus. To our knowledge such a sulcus is not present in any other diplodocid species, nor has it been reported from other sauropod taxa. It can thus be considered a true autapomorphy of *Kaatedocus siberi*. On the lateral aspect of the prezygapophyses of the CV 11 and 12 of SMA 0004, a second, parallel ridge – dorsal to the pre-epipophysis – progresses horizontally and subparallel to the articular facets. This second ridge is less conspicuous than the pre-epipophysis. The upper ridge is confluent with the sprl posteriorly. As in CV 10, the sdf in CV 11 to 13 forms a deep cavity posteroventrally to the pre-epipophysis and the second ridge. The pre-epipophysis extends slightly anterior to the prezygapophysis and forms the anteriormost point of CV 11 to 13, while it gets slightly reduced in CV 14. Its anterior end unites with the prdl in CV 11 and 12, but remains independent in CV 13 and 14. Ventrally, the prezygapophysis is supported by strong cprl that remain undivided in CV 11, but show shallow centroprezygapophyseal lamina fossae in CV 12 to 14. The relative strengths of the medial and lateral branches of the cprl change from one vertebra to the other. In all three elements, the right cprl is more divided than the left, forming a left–right asymmetry. In CV 12 both branches are subequally developed, CV 13 has a stronger medial, and CV 14 a slightly better built lateral portion.

The division of the cprl was considered synapomorphic for Diplodocidae (Wilson 2002; Remes 2007; Sereno *et al*. 2007; Whitlock 2011a). Medially, the prezygapophyses are united by a thin tprl.

Whereas the sprl is interrupted at the base of the prezygapophysis in CV 11, it can be followed without problems throughout its entire length in the more posterior elements. The sprl gets progressively more curved from CV 11 to 14, and almost describes a U-shape in last two preserved elements. At its dorsal end, just below the neural spine summit, the sprl develops a rounded (CV 13 and 14) to rather pointed (CV 11 and 12) anterior bulge, similar to the state in *Diplodocus carnegii* CM 84 and *Barosaurus lentus* YPM 429 (Hatcher 1901; pers. obs. 2011). This anterior bulge can thus be considered a diplodocine synapomorphy.

Between the two metapophyses of the divided posterior neural spine of SMA 0004 the true neural spine is atrophied into a median tubercle. Each one of the metapophysis summits is much longer than broad. In lateral view, the summit is topped by a horizontal table. The metapophyses are laminar, and very compressed transversely. Whereas the lateral surface of the posterior neural spines does not bear such distinct, dorsoventrally long cavities as in the mid-cervical vertebrae, CV 11 still exhibits a small anterior indentation, dorsal to the uppermost extension of the median tubercle (Fig. 10, C2). This depression is somewhat set back from the sprl and thus is probably not homologous to the elongated fossa on the posteroventral to the sprl of the previous elements. More anteriorly, where the homologous structure would be expected, there is a much less defined and more rounded depression in CV 11, which can also be observed in the more posterior elements. The distal end of the metapophyses is laterally marked by a rugose surface that extends ventrally to a height just below the anterior bulge of the sprl. On their medial side the metapophyses of all posterior cervical vertebrae bear a ridge formed by a step like structure that extends to meet the median tubercle. While the spine summit migrates anteriorly, the median tubercle remains located above the middle of the centrum in lateral view. The ridge on the medial surface of the metapophyses therefore changes its orientation within the series. In CV 11 and more anterior elements, it extends anteroventrally to meet the posterior extension of the median tubercle. In CV 12, it is oriented vertically, and in CV 13 and 14, it is anteriorly inclined and connects to the anterior end of the median tubercle.

The diapophysis of the posterior cervical vertebrae is situated in the second quarter of the vertebra, above the posterior portion of the anterior pneumatic fossa. It is axially long but not very projected transversely and bends ventrally towards its lateral end, forming a gentle curve. The articular end projects slightly anteroventrally in CV 11 and 12, and vertically in CV 13 and 14. The diapophysis unites four laminae: the prdl anterodorsally, the podl posterodorsally, the acdl anteroventrally, and the pcdl posteroventrally. Whereas the pcdl as well as the prdl are oriented relatively straight horizontally in CV 11 to 13, CV 14 has considerably elevated diapophyses and prezygapophyses. Both the prdl and pcdl are thus distinctly anteriorly inclined. In CV 13 and 14, the prdl borders a deep prcdf together with the cprl medially and the acdl posteriorly. The prcdf is further marked by one (CV 13) or two (CV 14) distinct depressions on its medial wall. In all posterior cervical vertebrae, the acdl originates on the centrum and proceeds subparallel with the podl until it reaches the centre of the ventral surface of the diapophysis. There it bends to extend vertically outwards onto the diapophysis–tuberculum complex, so that the dorsal portion of the latter has a subtriangular cross section. No posterior projection is present in CV 11 and 12, and only a short but pointed spur or a slight rugosity are visible in the left diapophysis of CV 14 and the right of CV 13, respectively. The pcdl and the podl of CV 11 have a small vertical lamina that unites them, with the free edge facing posteriorly. This accessory lamina thus subdivides the pocdf into two smaller cavities. The more posterior elements do not show this feature, but exhibit short ridges originating around midlength on the dorsal face of the pcdl and extending vertically before disappearing on the lateral wall of the neural canal. The cdf of CV 11 to 14 is deeply invaginated, and marked by a progressively more distinct, small cavity at its dorsomedial acute corner.

The postzygapophyses form a V in posterior view and are strongly concave transversely. Dorsally to the postzygapophyses the epipophysis is confluent with the spol, as well as with a horizontal ridge connecting to the podl that is subparallel to the postzygapophyseal facet. The epipophysis forms a pointed posterior projection overhanging the zygapophysis in CV 11 to 13, but not in CV 14. The articular facets are distinct from the postzygapophyseal process dorsally, but grade into the tpol ventrally. The latter connects the two postzygapophyses ventrally above the midline of the neural canal, but projects posteriorly and terminates above the posterior edge of the centrum. It forms a U-shaped notch in lateral view, with the rounded portion facing anteriorly, and the two parallel sides being represented by the horizontal dorsal centrum and the posteriorly projecting tpol. The course of the spol is bipartite in CV 11 and 12, being straight along most of its extent in both lateral and dorsal view, until it curves dorsally (in lateral view) to support the horizontal table of the neural spine summit. In CV 13 and 14, the spol extends anteriorly in a very acute angle to the podl, to a position above the posteriormost extension of the pcdl, at about half of its length. There it curves more dorsally and becomes somewhat convex. Below the summit table, it bends straight dorsally as in CV 11 and 12.

Cervical ribs

The ribs are well fused to the vertebra, which renders the distinction between the tuberculum and diapophysis difficult. The cervical ribs are usually shorter than the centrum

length. However, in CV 3, 12 and 14, they protrude slightly beyond the posterior centrum wall (Fig. 8, C2, C3; Fig. 10, B2, B3). Due to the dorsoventrally higher posterior than the anterior end of the vertebral centrum, the ribs – although protruding somewhat ventrally at the parapophyses – do not increase the maximum height of the vertebrae to a significant degree. However, overhanging cervical ribs are absent in other diplodocid taxa apart from *Dinheirosaurus.* The latter and *Kaatedocus siberi* can thus be considered plesiomorphic for this trait. Whereas in the anterior cervical ribs the tuberculum is inclined distinctly posteriorly to meet the diapophysis, in mid-cervical and posterior cervical ribs the inclination decreases and CV 13 and 14 have an almost vertical diapophysis–tuberculum complex. The proximal end of the tuberculum is slightly subtriangular in cross section initially but becomes transversely flattened ventrally. The tuberculum projects at least three times more than the capitulum which is axially long, dorsoventrally short and moderately projected medially. All cervical ribs have a pronounced anterior projection that represents from about one-fifth of the length of the rib in CV 3, 7 and 11, to approximately one-third in CV 5 and 8. The rib shaft is often somewhat deformed but appears to be slightly bowed, with the anterior and posterior extremes curving dorsally and often ending above the ventralmost point of the posteroventral flanges of the centrum. In anterior to mid-cervical ribs the shaft is slender and subcircular to subtriangular in cross section with the longer side facing medially, and the shorter sides laterodorsally and ventrolaterally. Posterior elements are more robust and mediolaterally flattened. The depth of the shaft is constant in lateral view, so its dorsal and ventral rims are subparallel until they taper at their ends. The only exceptions are CV 8 to 10 where the cervical ribs show a distinct dorsoventral expansion shortly after midlength, before they taper towards their posterior extreme. A few cervical ribs show special morphologies that do not appear on other elements: cervical rib 4 exhibits a distinct bend and slightly rugose area that probably represents reactive bone growth after a fracture of the cervical rib shaft (see Online Supplementary Material). Furthermore, the lateral side of cervical rib 11 exhibits two slot-like depressions on the right ventrally to the tuberculum (Fig. 10, C2, arrows). These might represent bite marks, which would be the only ones in the specimen.

Phylogenetic analysis

The phylogenetic analysis is based on Whitlock (2011a; modified by Mannion *et al.* 2012), with the addition of some characters from Upchurch *et al.* (2004b), Harris (2006c), Lovelace *et al.* (2007), Whitlock & Harris (2010), Whitlock (2011a) and 23 newly defined characters based on the description of SMA 0004 (see Online Supplementary Material). Previously performed preliminary analyses using unchanged existing matrices (Upchurch *et al*. 2004b; Harris 2006c; Whitlock 2011a) recovered SMA 0004 consistently inside Diplodocinae (ET, unpublished). Therefore, several changes concerning terminal taxa were introduced. The incomplete basal diplodocoid *Haplocanthosaurus* and all rebbachisaurids except for *Limaysaurus* were omitted as their positions in the past have been respectively controversial (Wilson 2002; Upchurch *et al*. 2004a) or poorly resolved (Mannion *et al.* 2012). The relatively complete *Nigersaurus* and *Brachytrachelopan* were deleted from the matrix because they represent very specialized forms within Rebbachisauridae and Dicraeosauridae, respectively, and therefore bear little additional information on diplodocid ingroup relationships. Furthermore, outgroup taxa with respect to Diplodocoidea were reduced to the very well-known basal macronarian *Camarasaurus* and the non-neosauropod eusauropod *Omeisaurus.* Within Diplodocidae, the multi-species genera *Apatosaurus* and *Diplodocus* are considered monophyletic, which was supported for *Apatosaurus* in the specimen-based phylogenetic analysis of Upchurch *et al.* (2004b). Additional coding for modified and new characters of *Apatosaurus* was based on *A. louisae*, as this species is the most complete and best reported in the genus. In contrast, *Diplodocus* is still pending a detailed review of its species-level taxonomy. As this would exceed the scope of the current study, we have adopted the coding of the original studies for the unmodified characters (with some changes mentioned and explained in the Online Supplementary Material) but concentrate on *D. carnegii* in the coding for the modified and new characters. The final analysis thus includes 14 taxa and 234 characters. The sources for the modified scoring in original characters as well as the coding in the modified and new characters are given in Online Supplementary Material Table S1.

Two different analyses were conducted using the heuristic search in WinClada 1.00.08 with 50 replicates. In the first, all multistate characters were treated as unordered, whereas in the second run, nine of the total 22 multistate characters were ordered, seven based on the fact that they describe either continuous ratios or vertebral counts. The remaining two ordered characters are 34 and 97. The former describes the laterally projecting spur, which is most probably an extension of the dorsoventrally elongated lateral ridge (character state 1) present in, for example, *Diplodocus*. Character 97 describes the bifurcation of the cervical vertebrae, which starts in anterior elements in *Diplodocus* but more posteriorly in SMA 0004 and other taxa. The bifurcation is considered to happen continuously from the back to the front (Woodruff & Fowler 2012) during ontogeny. Basing on Haeckel's rule that phylogeny recapitulates ontogeny, the development of this bifurcation in adult specimens should replay this continuous change, and an ordering of this character therefore appears reasonable.

Both analyses produced the same results (Fig. 11). *Kaatedocus siberi* is therefore recovered within Diplodocinae, as sister group to a polytomy including *Tornieria africana* + *Barosaurus lentus* + *Diplodocus*. The recovered Nelsen

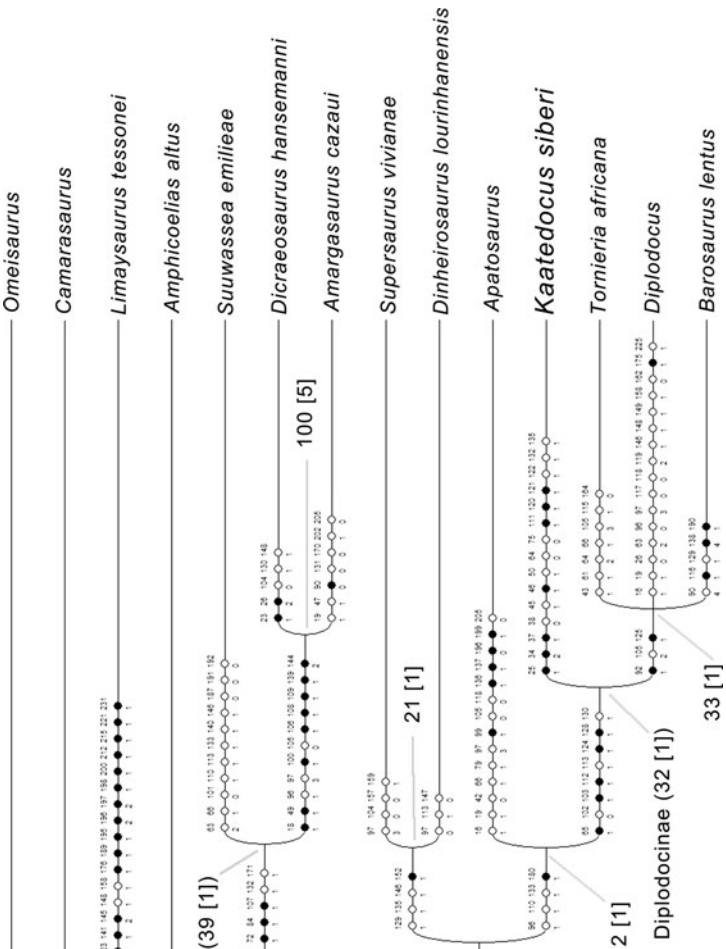

Figure 11. Nelsen Consensus tree obtained from a heuristic search in WinClada (six most parsimonious trees; tree length = 388; CI = 64%; RI = 57%). Dots indicate ambiguous (white) and unambiguous (black) synapomorphies, and autapomorphies of the respective clade. The corresponding character number and scoring is indicated above and below the dots, respectively. Main clades are indicated by their name, and bootstrap as well as Bremer Support values are given for each node (Bremer Support in square brackets). *Kaatedocus siberi* is resolved as Diplodocinae more basal than *Tornieria africana*, *Barosaurus lentus* and *Diplodocus*.

consensus tree (based on six equally parsimonious trees retained in the original analysis) has a length of 388 steps, a Consistency Index of 64%, and a Retention Index of 57%.

Discussion

Comparison with other diplodocids

The Morrison Formation has produced the most diverse diplodocid fauna worldwide, including at least 12 taxa currently considered valid (see above). The vast majority of described taxa of this clade come from this Upper Jurassic formation, with only a few exceptions from Europe and Africa. The abundance of diplodocids and their diversity was recognized in the early years of palaeontology (Marsh 1877, 1878, 1890; Osborn 1899; Hatcher 1901; Holland 1915; Gilmore 1932, 1936), and new diplodocid or closely related taxa are still being recovered (Jensen 1985; McIntosh *et al.* 1992; Filla & Redman 1994; Harris & Dodson 2004).

Although several diplodocid species have been reported previously, specimen SMA 0004 can be undoubtedly distinguished from all of these (Fig. 11). The present phylogenetic analysis recovers 15 autapomorphies in SMA 0004, seven of them unambiguous (but see detailed discussion below). It can be confidently identified as diplodocid, due to the hooked posterior process of the prefrontal, the absence of a contact between the squamosal and the quadratojugal, the 14–15 cervical vertebrae, and the divided cprl in mid- and posterior cervical vertebrae (Upchurch 1995, 1998; Wilson 2002; Harris 2006c; Mannion *et al.* 2012; Whitlock 2011a). It is easily distinguishable from *Apatosaurus* by its more slender cervical vertebra, and cervical ribs that do not project far ventrally (Gilmore 1936; Upchurch *et al.* 2004b). An attribution of SMA 0004 to *Supersaurus* can be excluded due to its small size and the much less elongated mid-cervical centra (see Lovelace *et al.* 2007). *Dinheirosaurus* differs from *Kaatedocus siberi* as it appears to have unbifurcated neural spines, as well as a groove posterior to the parapophyses, marking the ventrolateral edges of the posterior cervical centra (Mannion *et al.* 2012) – both local autapomorphies of *Dinheirosaurus* within Diplodocidae. *K. siberi* differs from the more derived *Barosaurus*, *Tornieria* and *Diplodocus* in the absence of a small, anteroposteriorly elongate fossa posteroventral and separate from the main pleurocoel, relatively short mid-cervical vertebrae, and the lack of a vertical accessory lamina posterior to the sprl of posterior cervical vertebrae (unknown in *Tornieria*).

As some of the distinguishing features have previously been interpreted as ontogenetic, a more detailed comparison is appropriate between SMA 0004 and more derived diplodocine species (including *Tornieria africana*, *Diplodocus longus*, *D. carnegii*, *D. hayi* and *Barosaurus lentus*). Whereas *T. africana* was found in Tanzania (Fraas 1908; Sternfeld 1911; Remes 2006), all species of *Diplodocus* as well as *B. lentus* are only known from the Morrison Formation (Marsh 1878, 1890; Hatcher 1901; Holland 1924). The two latter genera were reported from the Howe Quarry by Brown (1935) but this identification was not accompanied or followed by a thorough scientific analysis and description. Two well-preserved necks from the AMNH 1934 excavation at Howe Quarry are tentatively identified as *Barosaurus* (AMNH 7530 and 7535; Michelis 2004). Both are of approximately the same size as SMA 0004, show disarticulated skull material, but have never been described in detail (Brown 1935; Michelis 2004). Other diplodocine specimens comparable in size to SMA 0004 are very rare. The only other well-described specimen is a juvenile *Diplodocus* skull (CM 11255; Whitlock *et al.* 2010).

Comparison of *Kaatedocus siberi* with *Barosaurus lentus* and *Tornieria africana* is hampered due to little overlap in the incomplete reported specimens, which is probably also the reason for the relatively low bootstrap values in the recovered phylogenetic tree (see Fig. 11). Both of these taxa show very elongated cervical vertebrae (McIntosh 2005; Remes 2006). Wedel *et al.* (2000) reported an increase of the EI in *Apatosaurus* of 35–60%, comparing very young individuals to adults. SMA 0004 has an elongation index about 82% of that of *Diplodocus carnegii* CM 84, and 66% of *B. lentus* AMNH 6341 (Hatcher 1901; Wedel *et al.* 2000; McIntosh 2005). The increase during ontogeny would thus be 22% to reach the ratio in *Diplodocus*, or 52% for *Barosaurus*. As a very young age for SMA 0004 can be excluded due to the complete neurocentral fusion, the ratio has to be lower than that spanning practically the entire ontogeny in *Apatosaurus* (Wedel *et al.* 2000). An allometric growth strong enough to reach the elongation of *Barosaurus* or *Tornieria* thus appears improbable. Furthermore, the braincase identified as *T. africana* (MB.R.2386; Remes 2006) can be distinguished from SMA 0004 by the curved instead of straight dorsal edge of the posterolateral process of the parietal, the narrow width of the basal tubera and their U-shaped anterior border, as well as the presence of a foramen in the notch separating them (Janensch 1935; Remes 2006). Besides having a much more elongated centrum, the only preserved cervical vertebra of *T. africana* (MB.R.3816; Remes 2006) does not show a ventral ridge (Remes 2006). Of the possible additional *Tornieria* specimens, a dentary (MB.R.2347) is less squared than that of *Diplodocus* CM 11161 but also less rounded than that of SMA 0004. However, assignment of MB.R.2347 to *T. africana* is uncertain (Remes 2009), and therefore this difference remains doubtful. Besides the cervical vertebral elongation and the snout shape, none of the aforementioned characters have previously been interpreted as being affected by ontogenetic changes in sauropods. These characters are thus interpreted to be sufficiently distinct and independent from ontogeny that a generic separation from *T. africana* is reasonable for *K. siberi*.

A separation of *Kaatedocus siberi* from *Barosaurus lentus* is equally well supported. Apart from the improbable enormous allometric growth necessary for the cervical vertebrae of SMA 0004 to reach the elongation index of *B. lentus* (McIntosh 2005), three more morphological characters can be put forward to distinguish these two taxa (plus the unambiguous autapomorphies of *K. siberi*). *B. lentus* YPM 429 exhibits a bifurcate anterior end of the pcdl, and postzygapophyses that terminate anterior to the posterior margin of the posterior cervical centra (Lull 1919; pers. obs. 2011). Furthermore, the ventral keels in the cervical vertebrae of the *B. lentus* holotype YPM 429 show a quite different morphology from the single anterior ridge in SMA 0004: in YPM 429 two crests extend obliquely from between the parapophyses posterolaterally to unite with the posteroventral flanges (Lull 1919; pers. obs. 2011). Adding the recovered autapomorphies of *K. siberi*, a generic distinction from *Barosaurus* can be justified.

Diplodocus is the most abundant diplodocine sauropod in the Morrison Formation. The initial provisional identification of SMA 0004 as *Diplodocus* by Ayer (2000) shows that a separation from this taxon is the most difficult. *Diplodocus* is the only diplodocine for which a juvenile skull has been reported (CM 11255), and this specimen superficially looks much like SMA 0004 (Whitlock *et al.* 2010). Differences between CM 11255 and *Diplodocus* skulls of older individuals (CM 3452 and 11161) include a rounder snout shape, maxillary teeth that reach further posteriorly, and a relatively larger orbit (Whitlock *et al.* 2010). These are traits that also distinguish *Kaatedocus siberi* from *Diplodocus*. More detailed comparisons of SMA 0004 with the subadult and juvenile *Diplodocus* skulls CM 3452 and 11255 show that some of the recovered autapomorphies of *K. siberi* are actually shared with the latter specimens, and might therefore be ontogenetic. These include the lateral spur on the lacrimal, the ridge on the paroccipital processes, and the straight orientation of the anterior edge of the basal tubera, traits present in both CM 3452 and 11255 but absent in adult *Diplodocus* skulls (AMNH 969; CM 11161; USNM 2672, 2673; pers. obs. 2011). Furthermore, the shallow fossa medial to the pterygoid ramus is also observable in CM 3452, but neither in CM 11255 nor in the abovementioned adult specimens (pers. obs. 2011). Other more widespread features shared with the juvenile and absent in the adult stages are the prefrontal that does not reach far posteriorly, and relatively more elongate frontals in CM 3452 and SMA 0004 (both unknown in CM 11255). The shallow groove that accommodates both the subnarial and the anterior maxillary foramen in CM 3452, 11161, as well as USNM 2672, is lacking in CM 11255 and SMA 0004 (Whitlock *et al.* 2010; pers. obs. 2011). The basipterygoid processes of SMA 0004 resemble more their corresponding structures in CM 11255, than in CM 3452 and 11161. In the latter, subadult to adult specimens, the processes are straight along their entire extent, and without a curved shelf that connects the base of the processes. In SMA 0004 and CM 11255, such a shelf is present, and throughout its extent, it keeps the processes subparallel in ventral view, before they curve laterally.

Other osteological features in SMA 0004 more closely resemble adult *Diplodocus* skulls than CM 11255. The squamosal of CM 11255 was shown to have an elongated anterior process that almost contacts the quadratojugal, whereas in adult skulls (and also in SMA 0004) these two bones are well separated (Whitlock *et al.* 2010; CM 11161; USNM 2672, 2673, pers. obs. 2011). Furthermore, the dorsal margin of the quadrate is concave in lateral view in CM 11255 but fairly straight in adult *Diplodocus* and *Kaatedocus siberi* (Whitlock *et al.* 2010; CM 11161; USNM 2672; pers. obs. 2011). The foramen present on the surangular in SMA 0004 appears to be lacking in CM 11255 (Whitlock *et al.* 2010), which indicates that in *Diplodocus* this foramen only develops during ontogeny.

Despite these similarities, several features present in SMA 0004 but absent in any *Diplodocus* skull indicate that the specimen described here is distinct from *Diplodocus.* The location of the frontal–parietal suture is more similar to its position in MB.R.2386 than in the *Diplodocus* skulls CM 11161 and 11255. Whereas in the *Diplodocus* skulls the suture is quite anteriorly placed with respect to the supratemporal fenestra, in both SMA 0004 and MB.R.2386 it is situated more posteriorly, around the centre of the opening in dorsal view (Remes 2006; Whitlock *et al.* 2010; pers. obs. 2011). The basal tubera are closer to the occipital condyle in SMA 0004, resembling more the state in *Suuwassea emilieae* ANS 21122 than in *Diplodocus* skulls CM 11161 and 11255 (Harris 2006a; Whitlock *et al.* 2010; pers. obs. 2011). There is no indication of a basipterygoid recess posterior to the basal tubera, a trait previously used to distinguish *Apatosaurus* from *Diplodocus* where such a recess is present (Wilson 2002; Whitlock *et al.* 2010). Additionally, SMA 0004 has a closed preantorbital fossa, similar to the state in *Dicraeosaurus hansemanni* MB.R.2336. As both *Apatosaurus* (CM 11162) and *Diplodocus* (including the juvenile CM 11255) show a distinct, open, oval preantorbital fenestra (Berman & McIntosh 1978; Whitlock *et al.* 2010), the retention of the plesiomorphic state in SMA 0004 can be considered taxonomically important. Furthermore, the tooth count in both the maxillae and the dentaries of SMA 0004 is higher than usual for *Diplodocus* (12–13 versus 9–11; Holland 1924; Barrett & Upchurch 1994; Calvo 1994; Whitlock *et al.* 2010; CM 11161, 11255, pers. obs. 2011), and appears equal to *Apatosaurus* CM 11162 (Berman & McIntosh 1978; Calvo 1994; pers. obs. 2011). Although a reduction in the number of teeth during ontogeny was proposed for *Camarasaurus* (McIntosh *et al.* 1996), the fact that CM 11255 shows the average number of teeth known in adult *Diplodocus* skulls indicates that the higher number in SMA 0004 most probably represents taxonomic diversity.

Possible diplodocid species from North America that were not included in this analysis are *Eobrontosaurus yahnahpin*, *Dystrophaeus viaemalae* and *Dyslocosaurus polyonychius*. However, *E. yahnahpin* has previously been interpreted as being a camarasaurid (Upchurch *et al*. 2004a), and thus most probably cannot be considered a diplodocine. Moreover, a distinction is easily made using the elongated neural spines in the anterior cervical vertebrae and the widely transversely projecting parapophyses (Filla & Redman 1994; P. Mannion, pers. comm. 2011). Comparisons with the other two taxa are impossible as they are very fragmentary and do not show any overlap (Cope 1877; McIntosh *et al*. 1992). Nonetheless, both remains are of larger animals than SMA 0004, and the difference appears too much to be explained by individual or sexual variation, even considering that SMA 0004 might still have been in the growth phase.

Autapomorphies of *Kaatedocus siberi*. The recovered autapomorphies of *Kaatedocus siberi* are discussed in detail below. As the discussion will show, some of these features are actually shared with farther related taxa that were not included into the present phylogenetic analysis, or with single specimens of included genera. They were therefore excluded or defined as local autapomorphies in the diagnosis of *K. siberi* (see above).

The U-shaped notch anteriorly between the frontals is recovered as an unambiguous autapomorphy. Diplodocid skulls usually have frontals that touch and fuse along their entire medial edge so that their anterior borders build one single straight line that connects to the nasals (Berman & McIntosh 1978; Wilson & Sereno 1998; Whitlock *et al*. 2010). In SMA 0004 the medial margin of the frontals curve laterally in their anterior half. A similar morphology can be seen in the partial skull of *Spinophorosaurus nigerensis* (Knoll *et al*. 2012), the holotype specimen of *Diplodocus hayi* HMNS 175 but in these specimens it is V- and W shaped, respectively, and not U-shaped as in *Kaatedocus siberi*. *D. hayi* has previously been doubted as congeneric with *Diplodocus* (Foster 1998). The difference in the frontals indicates that this hypothesis might prove to be correct, and its similarity to SMA 0004 could imply that HMNS 175 should group with *Kaatedocus siberi*. On the other hand several differences in the rest of the skull (e.g. orientation of the basipterygoid processes) and also the cervical vertebrae (e.g. dorsally expanded bifid neural spines already in anterior cervical vertebrae) preclude an assignment of SMA 0004 to *D. hayi* (Holland 1906, 1924; HMNS 175, pers. obs. 2010). The only partially conjoined frontals in SMA 0004 could also be interpreted as not entirely fused, and indicate an early juvenile age for the animal. However, embryonic skulls of the basal sauropodomorph *Massospondylus* show tightly appressed right and left frontals along their entire medial edge (Reisz *et al.* 2005), and the subadult skull of the titanosauriform *Bonitasaura salgadoi* has a frontal with an entirely straight medial margin (Gallina & Apesteguía 2011). This indicates that the outwards curve in the frontal of SMA 0004 is not an ontogenetic feature but is instead taxonomically significant and an unambiguous autapomorphy of *K. siberi*.

The laterally projecting spur is another unambiguous autapomorphy as recovered from the phylogenetic analysis. However, as stated above, the juvenile and subadult *Diplodocus* skulls CM 11255 and 3452 also show this feature, and therefore the influence of ontogeny cannot be ruled out, even though bony spurs and an increased development of ridges and crests are usually interpreted to be typical of older individuals (Varricchio 1997). Given that lacrimals are unknown in *Suuwassea*, *Supersaurus*, *Dinheirosaurus*, *Tornieria* and *Barosaurus*, a decision on the taxonomic importance of this morphological feature remains difficult. Furthermore, a similar spur is present in the camarasaurid SMA 0002 and some specimens mentioned in Madsen *et al.* (1995) as '*Camarasaurus*-like'. An interpretation of this lacrimal spur as locally autapomorphic within Diplodocoidea might thus be possible but must await further finds of definitively adult specimens of *K. siberi*, or juvenile skulls of more diplodocid taxa.

A third recovered unambiguous autapomorphy of *Kaatedocus siberi* is the small fossa present medially to the sheet-like pterygoid ramus of the quadrate. However, this character is also present in the subadult skull CM 3452. Its absence in both juvenile and adult *Diplodocus* specimens (CM 11161, 11255; USNM 2672, 2673; pers. obs. 2011) might imply that this feature is only developed in subadult specimens. A similar development can also be seen in the large quadrates belonging to the holotype of *Apatosaurus ajax* (YPM 1860), which also appears to be a juvenile to subadult specimen (McIntosh 1990). The development of such a medial quadrate cavity in subadult stages might thus be a synapomorphy of the entire Diplodocidae, and its interpretation as an autapomorphy of *Kaatedocus siberi* cannot be entertained with certainty at present.

The short anterior process of the squamosal appears as a local autapomorphy within Diplodocoidea. This process exceeds the posterior border of the orbit considerably in all known diplodocoid skulls, and even extends beyond the anterior orbital edge in the rebbachisaurs *Limaysaurus tessonei* and *Nigersaurus taqueti* (Calvo & Salgado 1995; Sereno *et al.* 2007). The retention of a short anterior process therefore appears to be a real local autapomorphy of *Kaatedocus siberi*.

The presence of a postparietal foramen is an ambiguous autapomorphy shared with *Dicraeosaurus*, *Amargasaurus* and *Suuwassea* in the present data matrix. It has thus been traditionally interpreted as a synapomorphy of Dicraeosauridae (Salgado & Bonaparte 1991; Remes 2009; Whitlock 2011a). Upchurch *et al*. (2004a) also reported a postparietal foramen in *Tornieria* but of the braincases found at Tendaguru, Tanzania, only MB.R.2387 shows such

a foramen (Janensch 1935; Remes 2009; pers. obs. 2011). MB.R.2387 has subsequently been identified as Flagellicaudata indet. as it could not be confidently referred to *Tornieria* based on the situation of the quarry, and because it shows a mix of dicraeosaurid and diplodocid characters (Remes 2009). The morphology of the foramen in SMA 0004 strongly resembles its corresponding structure in MB.R.2387, where it is considerably smaller than in *Suuwassea* and *Dicraeosaurus*. The presence of this foramen in SMA 0004 might also be due to incomplete fusion of the parietals in this specimen and thus be ontogenetic. However, the small *Diplodocus* skull CM 11255 does not show such a foramen, which is yet another characteristic that helps distinguish these two taxa. Awaiting a definitive taxonomic assignment of MB.R.2387, and finds of skulls of *Supersaurus*, *Dinheirosaurus* and *Barosaurus*, the postparietal foramen in *K. siberi* is provisionally regarded as a local autapomorphy within Diplodocidae.

The distinct oblique posterior ridges on the paroccipital processes of SMA 0004 are another recovered unambiguous autapomorphy, which is actually shared with the juvenile *Diplodocus* specimens (see above). A detailed analysis of the development and distribution of this character among juvenile to subadult individuals of different species has thus to be postponed until more material is found and described.

As with the postparietal foramen, the narrow and distinct sagittal nuchal crest is also a shared feature of *Kaatedocus siberi* and Dicraeosauridae (Salgado & Bonaparte 1991; Harris 2006a; Mannion *et al.* 2012; Whitlock 2011a). Furthermore, the indeterminate flagellicaudatan MB.R.2388 also exhibits a similar shape of the nuchal crest (Remes 2009). The state of this character is unknown in *Supersaurus*, *Dinheirosaurus* and *Barosaurus* as their skeletons are only known from postcranial material. The occurrence of such a distinct nuchal crest in SMA 0004 is the first reported for any diplodocid, and like the presence of a postparietal foramen, this feature was previously interpreted as a synapomorphy of the Dicraeosauridae. However, the low and broad nuchal crest of *Apatosaurus* and diplodocines more derived than *K. siberi* indicates that either the acquisition of this feature, or its loss, happened twice independently within Flagellicaudata. Interestingly, in contrast to the adult *Diplodocus* skull CM 11161, the juvenile *Diplodocus* CM 11255 does show a more developed sagittal nuchal crest (Whitlock *et al*. 2010). This implies that the high nuchal crest can also be an ontogenetic character that decreased in size during growth. This would mean that the well-developed crest in SMA 0004 could still become somewhat weaker and broader during ontogeny, and thus approach the state in *Tornieria africana* or *Diplodocus*. However, the development of the crest in CM 11255 does not equal its counterpart in SMA 0004, and such a pronounced change from a subadult to the adult stage seems improbable. Moreover, the opposite development has been shown to happen in *Massospondylus* and *Psittacosaurus* (Gow 1990; Varricchio 1997), and the closely related dicraeosaurids also show a well-developed crest in adult individuals. Therefore, even though it seems to be an ontogenetic feature in *Diplodocus* this might be different in *K. siberi*, of which the derived state can be considered locally autapomorphic within Diplodocidae.

The straight anterior edge of the basal tuber is shared with *Limaysaurus tessonei* in the present analysis. However, it is equally expressed in both juvenile and subadult *Diplodocus* (CM 11255, 3452, pers. obs. 2011), as well as *Nigersaurus taqueti* (Sereno *et al*. 2007). It might thus be that juveniles and subadult *Diplodocus* retain the plesiomorphic trait present in the more basal rebbachisaurs. The decision on how the appearance of this character in *Kaatedocus siberi* should be treated (ontogenetic character or retained plesiomorphy) should await future finds of adult *Kaatedocus* or juvenile basal diplodocid specimens.

The more rounded snout shape, with a premaxilla–maxilla index (PMI; see Whitlock 2011b for a detailed explanation) of less than 70% is shared with the juvenile specimen CM 11255 and CMC VP 8300 (Whitlock *et al.* 2010). With a PMI of 68%, *Kaatedocus siberi* is slightly beneath the border set by Whitlock (2011a) to define the plesiomorphic state. Based on the reconstructions of Whitlock (2011b), the PMI in SMA 0004 is very close to that of *Tornieria* (71%; Whitlock 2011b), which falls in the gap of the borders set for this character, but would rather group with the plesiomorphic taxa. *Suuwassea* is considered to have a slightly higher index of 74% by the same author, and is thus closer to the apomorphic state. These ratios are not included in this analysis as the reconstructions in Whitlock (2011b) are based on incomplete material. Nonetheless, they describe a general trend towards gradually more squared snouts during the evolution of Diplodocoidea, becoming extreme in *Nigersaurus*, *Apatosaurus* and *Diplodocus* (Whitlock 2011b). The retention of the plesiomorphic state in *K. siberi* and probably *Tornieria* therefore appears to be the exception to this rule, but the rounded snout in the juvenile *Diplodocus* skulls CM 11255 and CMC VP 8300 indicates that this might also be an ontogenetic feature (Whitlock *et al.* 2010). CM 11255 has a PMI of only 56%, which is even lower than in *Camarasaurus* or *Brachiosaurus* (Whitlock *et al*. 2010; Whitlock 2011b). Even though this might be partly due to transverse compression of the skull, it implies that juvenile *Diplodocus* develop the typical squared snout only during ontogeny. However, as *Tornieria* appears to show a similar value, a coding of *K. siberi* as plesiomorphic in this character can be justified, and can be regarded as local autapomorphy of *K. siberi*, and perhaps *Tornieria* too.

The anteriorly projecting pre-epipophysis that forms the anteriormost point of the entire mid-cervical vertebrae is another unambiguous autapomorphy in the phylogenetic analysis. Its distribution is unknown in *Supersaurus*,

Dinheirosaurus and *Tornieria*, but the preserved vertebrae in the first two of these taxa indicate that such a spur was probably not present. This feature was described as autapomorphic within Diplodocidae in *Australodocus* by Remes (2007), where it is very pronounced, and is also present in *Haplocanthosaurus* (Hatcher 1903). As *Australodocus* is currently considered a titanosauriform, the spur is herein interpreted to be a local autapomorphy of *K. siberi* within the clade uniting all diplodocoids more derived than *Haplocanthosaurus*. An alternative interpretation of this spur as a juvenile character is improbable as such traits usually develop late in ontogeny (Varricchio 1997).

The small, rugose tuberosity placed anterodorsally to the anterior pneumatic fossa on the lateral surfaces of the posterior cervical vertebrae represents another unambiguous autapomorphy of *Kaatedocus siberi*. Comparisons with various diplodocid specimens (e.g. *Apatosaurus* CM 3018; *Diplodocus* CM 84, DMNS 492, 1494, HMNS 175; *Barosaurus* AMNH 6341, YPM 429) indicate that this feature is unique in *K. siberi*. The only taxon with a similar trait is the basal dicraeosaurid *Suuwassea*, where the mid-cervical vertebrae bear a tubercle in the same position (ANS 21122, pers. obs. 2011). The fragmentary posterior cervical centra of ANS 21122 do not preserve this region in enough detail to discern their state. Therefore, an interpretation of this feature as local autapomorphy of *K. siberi* within Diplodocidae is relatively well supported, only lacking information about its distribution in *Supersaurus*, *Dinheirosaurus* and *Tornieria*. *Dinheirosaurus* ML 414 shows a fractured surface in this region, and the only preserved cervical vertebra of *Tornieria africana* is badly crushed, so the presence or absence of this tubercle cannot be determined in these taxa.

The sulcus posterior to the prezygapophyseal facets of the posterior cervical vertebrae is considered an additional unambiguous autapomorphy in the present analysis. Personal observations showed this trait to be absent in *Suuwassea*, *Apatosaurus*, *Diplodocus* and *Barosaurus* (AMNH 550; ANS 21122; CM 84, 94, 3018; YPM 429, 1860). In the holotype material of *Dinheirosaurus lourinhanensis* (ML 414) the prezygapophysis is partly covered by matrix and somewhat distorted but such a sulcus does not appear to be present. Furthermore, the detailed description of the cervical vertebrae of *Dicraeosaurus* (Janensch 1929) does not mention any similar structure in these taxa. In *Nigersaurus*, as a representative of a more distantly related diplodocoid, the distinct articular facets of the prezygapophysis are well offset from the prezygapophyseal process, but no transverse sulcus is present (Sereno *et al.* 2007). Neither the presence nor the absence of such sulci has previously been considered valuable for characterizing either adults or juveniles. This autapomorphy of *Kaatedocus siberi* can thus be assumed to unambiguous.

The posteriorly facing accessory lamina between the pcdl and the podl is shared between *Kaatedocus siberi* and *Dinheirosaurus*. However, such a lamina is also present in the *Apatosaurus* specimens UW 15556, YPM 1840, 1860 and 1861 (Gilmore 1936; Wedel & Sanders 2002; pers. obs. 2011). This character is thus not considered an autapomorphy of *K. siberi*.

The narrowly diverging neural spines of SMA 0004 resemble more closely the state in dicraeosaurids than in diplodocids. The possibility cannot be excluded that this character was affected and exaggerated by taphonomy; therefore, a question mark has to be placed over its designation as a local autapomorphy within Diplodocidae. However, as the diapophysis of CV 14 in particular does not seem to be highly deformed, a narrower angle between the metapophyses can still be assumed. On the other hand, the supposed *Barosaurus* sp. CM 11984 also exhibits less widely diverging neural spines compared to other diplodocids. A decision on the validity of this autapomorphy is thus not possible yet.

The cervical ribs that in some vertebrae exceed the posterior end of the centra are another ambiguous autapomorphy of *Kaatedocus siberi*. The only other diplodocoids with the same trait are *Supersaurus* and *Dinheirosaurus*, which are recovered as a sister group to Diplodocidae in the present phylogenetic analysis (contrary to previous analyses, see below). Elongated cervical ribs were also reported in *Eobrontosaurus yahnahpin*, the taxonomic affinity of which has yet to be resolved. At present, this feature thus represents a local autapomorphy within Diplodocidae.

To summarize, *Kaatedocus siberi* can be confidently identified by three general unambiguous autapomorphies: (1) the U-shaped notch between the frontals; (2) the lateral rugose tubercle on anterodorsal corner of posterior cervical centra; and (3) the sulcus bordering the prezygapophyseal facets posteriorly in posterior cervical vertebrae. Furthermore, the diagnosis is strengthened with local autapomorphies or retained plesiomorphies (see above).

Phylogenetic implications

In the majority of the phylogenetic analyses on Sauropoda, the clade Diplodocidae was well resolved and easily distinguishable from other clades. This was mainly due to the inclusion of a limited number of diplodocid taxa, using only the best-known genera *Apatosaurus*, *Diplodocus* and *Barosaurus* (Upchurch 1995, 1998; Wilson & Sereno 1998; Wilson 2002, 2005; Upchurch *et al.* 2004a). Recent studies have looked in detail at the intra-relationships of this group, including more incomplete taxa, even single specimens such as *Supersaurus*, '*Seismosaurus*' (Lovelace *et al.* 2007), and different apatosaur species (Upchurch *et al.* 2004b). Only two detailed phylogenetic analyses have included a larger set of ingroup taxa, representing the most inclusive diplodocid phylogenies published to date (Mannion *et al*. 2012; Whitlock 2011a). Although Whitlock (2011a) helped in resolving uncertainties within the more basal diplodocoid clade Rebbachisauridae, Diplodocidae

Figure 12. Life reconstruction of the skull of *Kaatedocus siberi*. Note the lateral spur on the lacrimal and the palpebral element covering the orbit. Illustration by Davide Bonadonna (Milan).

was not fully resolved, with *Dinheirosaurus*, *Tornieria* and a clade comprising the classical diplodocines *Diplodocus* and *Barosaurus* forming a trichotomy. Mannion *et al.* (2012), based on Whitlock's (2011a) matrix, redescribed *Dinheirosaurus* in detail and were therefore able to update and correct some character states used in the earlier study. *Dinheirosaurus* was recovered as a sister taxon to *Supersaurus*, and together they form the most basal subclade within Diplodocinae, followed by *Tornieria* and (*Diplodocus* + *Barosaurus*). The addition of *Kaatedocus* and several new characters to the matrix corroborates this result in parts (Fig. 11): in the Nelsen consensus tree, the clade comprising *Dinheirosaurus* and *Supersaurus* is recovered more basal than *Apatosaurus* – and would therefore form the basalmost clade within Diplodocidae (following the definitions recommended by Taylor & Naish 2005). This corroborates the assumption of Mannion *et al.* (2012) that the assignment of *Dinheirosaurus* to Diplodocinae has still to be considered uncertain, as this taxon shares a number of traits with more basal diplodocoids. However, the low bootstrap values imply that more detailed studies are still needed in order to resolve diplodocid phylogeny in a convincing way. The fact that *Kaatedocus* exhibits features previously identified as dicraeosaurid synapomorphies indicates that some of them were actually already present in basal flagellicaudatans and subsequently lost in diplodocids other than *Kaatedocus*.

The basal position of *Kaatedocus siberi* in the diplodocid clade is consistent with the low stratigraphical position (Fig. 2), considered older than most sauropod occurrences in the Morrison Formation. *K. siberi* thus makes a nice example of Cope's Rule as well, as a small sized, more basal taxon, compared with the large, advanced diplodocines *Barosaurus* and *Diplodocus*. However, as already mentioned, the stratigraphy of the northern exposures of the Morrison Formation is ambiguous, and long distance correlation with the better known southern sites is difficult (Turner & Peterson 1999; Trujillo 2006). As the few reported specimens from northern Wyoming or Montana comprise previously unknown or rare species (Wilson & Smith 1996; Harris 2006c), long distance correlation by proposed faunal zones (see Foster 1998; Turner & Peterson 1999) appears difficult as well. The recent descriptions of new taxa from these areas (e.g. Harris & Dodson 2004; this study) therefore highlights the importance of a more detailed exploration and analysis of the northern Morrison Formation, both for a better understanding of diplodocid phylogeny and stratigraphical correlation of the various fossil sites and faunal changes within the formation.

Skull reconstruction

Some of the skull elements bear features that are reported for the first time in diplodocid sauropods. The majority of these characters would have been hidden *in vivo*, like the posterior expansion of the nasal opening, the anteriorly restricted squamosal, and the morphology of the braincase and the quadrate. However, the lacrimal spur and the rugose lateral surface of the frontal, which indicates the presence of a palpebral element, are traits that affected the outward aspect of the living *Kaatedocus*. Fig. 12 shows a skull reconstruction, undertaken in cooperation with the Italian artist Davide Bonadonna, showing these features.

Conclusions

Kaatedocus siberi is a new diplodocid sauropod from the little-known northern exposures of the Upper Jurassic Morrison Formation of Wyoming, USA. It was found at the historic Howe Quarry, relatively low in the stratigraphy, and therefore fills both a spatial as well as temporal gap from which only few sauropod specimens have been reported. *K. siberi* represents a basal diplodocine, and forms the sister taxon to a clade including *Tornieria africana*, *Barosaurus lentus* and the multi-species genus *Diplodocus*. With its smaller size compared to the more derived taxa, it is an example of Cope's Rule, which predicts a body size increase during evolution. The holotype comprises a disarticulated but nearly complete skull and an associated cervical vertebral column (including the first record of a proatlas in diplodocid dinosaurs), and is interpreted as a subadult individual. Newly identified, possibly ontogenetic features include a shallow excavation on the quadrate shaft, medial to the pterygoid ramus, oblique ridges on the external side of the paroccipital processes, and a straight anterior margin of the basal tubera in ventral view. *K. siberi* furthermore shares characters that were previously interpreted as dicraeosaurid synapomorphies. The presence of a postparietal foramen, as well as the narrow but distinct sagittal nuchal crest, therefore probably represents the plesiomorphic state in Flagellicaudata. An updated phylogenetic analysis recovers the clade uniting *Supersaurus* and *Dinheirosaurus* as the most basal Diplodocidae.

The highly rugose lateral margins of the frontal are considered equivalent to the attachment sites of palpebral bones on frontals in ornithischian dinosaurs. This is the first such interpretation for sauropod dinosaurs, and a skull reconstruction of *Kaatedocus siberi* was therefore attempted, which shows a palpebral element covering the eye anterodorsally. SMA 0004 is the only specimen from the historic Howe Quarry to be completely described and properly identified to date. The fact that it represents a new diplodocid taxon highlights the importance of this site, but further studies are needed to understand better the implications for diplodocid phylogeny as well as faunal changes in the Morrison Formation through space and time.

Acknowledgements

We thank Hans-Jakob Siber (SMA) for the organization of the excavation, collection, preparation and curation of the holotype specimen, and for the opportunity to study it. We are indebted to Davide Bonadonna (Milan, Italy) who provided the highly accurate skull reconstruction. Comments on an early version of the manuscript by Phil Mannion, John Whitlock and Paul Upchurch improved the quality of this paper considerably. Thomas Bollinger (SMA), Amy Henrici, Matthew Lamanna (CM), Ralf Kosma, Ulrich Joger (SNMB), Carl Mehling and Mark Norell (AMNH) provided access to collections. Michael Taylor and Mathew Wedel shared pictures and more detailed information about their work. José Carballido and Phil Mannion shared information about unpublished studies. Laura Redish was of great help concerning the Crow/Absaroka language and the naming of the new genus. Many thanks go to Esther Premru and Ben Papst for the preparation of the specimen and the quarry map, and the reconstruction of the skull, to Lara Couldwell (ML) and Holly Barden (University of Manchester) for correcting the English, as well as to João Marinheiro and Matthias Meier for assistance during the description. Emanuel Tschopp is supported by Fundação para a Ciência e a Tecnologia doctoral fellowship SFRH/BD/66209/2009 (Ministério da Ciência, Tecnologia e Ensino superior, Portugal). Travel subsidies in order to see the collection of the Museum für Naturkunde, Berlin, were kindly provided by a Synthesys grant (DE-TAF-1150) to ET.

Supplementary material

Supplementary material is available online DOI: 10.1080/14772019.2012.746589

References

Ayer, J. 2000. *The Howe Ranch Dinosaurs*. Sauriermuseum Aathal, Aathal, 96 pp.

Balanoff, A. M., **Bever, G. S.** & **Ikejiri, T.** 2010. The braincase of *Apatosaurus* (Dinosauria: Sauropoda) based on Computed Tomography of a new specimen with comments on variation and evolution in sauropod neuroanatomy. *American Museum Novitates*, **3677**, 1–32.

Barrett, P. M. & **Upchurch, P.** 1994. Feeding mechanisms of *Diplodocus*. *Gaia*, **10**, 195–203.

Berman, D. S. & **McIntosh, J. S.** 1978. Skull and relationships of the Upper Jurassic sauropod *Apatosaurus* (Reptilia, Saurischia). *Bulletin of the Carnegie Museum of Natural History*, **8**, 1–35.

Birkemeier, T. 2011. Neurocentral suture closure in *Allosaurus* (Saurischia: Theropoda): sequence and timing. *Journal of Vertebrate Paleontology, Program and Abstracts*, **2011**, 72A.

Bonaparte, J. F. 1986. The early radiation and phylogenetic relationships of the Jurassic sauropod dinosaurs, based on vertebral anatomy. Pp. 247–258 in K. Padian (ed.) *The Beginning of the Age of Dinosaurs*. Cambridge University Press, Cambridge.

Bonaparte, J. F. & **Mateus, O.** 1999. A new diplodocid, *Dinheirosaurus lourinhanensis* gen. et sp. nov., from the Late Jurassic beds of Portugal. *Revista del Museo Argentino de Ciencias Naturales*, **5**(2), 13–29.

Brown, B. 1935. Sinclair dinosaur expedition, 1934. *Natural History*, **36**, 2–15.

Calvo, J. O. 1994. Jaw mechanics in sauropod dinosaurs. *Gaia*, **10**, 183–193.

Calvo, J. O. & **Salgado, L.** 1995. *Rebbachisaurus tessonei* sp. nov. a new sauropod from the Albian-Cenomanian of Argentina; new evidence on the origin of the Diplodocidae. *Gaia*, **11**, 13–33.

Carabajal, A. P., **Coria, R. A.** & **Chiappe, L. M.** 2008. An incomplete Upper Cretaceous titanosaur (Sauropoda) braincase: new insights on the dinosaurian inner ear and endocranium. *Cretaceous Research*, **29**, 643–648.

Christiansen, N. A. & **Tschopp, E.** 2010. Exceptional stegosaur integument impressions from the Upper Jurassic Morrison Formation of Wyoming. *Swiss Journal of Geosciences*, **103**, 163–171.

Cope, E. D. 1877. On a dinosaurian from the Trias of Utah. *Proceedings of the American Philosophical Society*, **16**(99), 579–584.

Dodson, P., **Behrensmeyer, A. K.**, **Bakker, R. T.** & **McIntosh, J. S.** 1980. Taphonomy and paleoecology of the dinosaur beds of the Jurassic Morrison Formation. *Paleobiology*, **6**(2), 208–232.

Filla, B. J. & **Redman, P. D.** 1994. *Apatosaurus yahnahpin*: a preliminary description of a new species of diplodocid dinosaur from the Late Jurassic Morrison Formation of Southern Wyoming, the first sauropod dinosaur found with a complete set of "belly ribs". Pp. 159–178 in G. E. Nelson (ed.) *The Dinosaurs of Wyoming. Wyoming Geological Association 44th Annual Field Conference Guidebook*. Wyoming Geological Association, Casper.

Foster, J. R. 1998. *Aspects of vertebrate paleoecology, taphonomy, and biostratigraphy of the Morrison Formation (Upper Jurassic), Rocky Mountain region, western United States*. Unpublished PhD dissertation, University of Colorado, 466 pp.

Fraas, E. 1908. Ostafrikanische Dinosaurier. *Palaeontographica*, **15**, 105–144.

Gallina, P. A. & **Apesteguía, S.** 2011. Cranial anatomy and phylogenetic position of the titanosaurian sauropod *Bonitasaura salgadoi*. *Acta Palaeontologica Polonica*, **56**, 45–60.

Gillette, D. D. 1991. *Seismosaurus halli*, gen. et sp. nov., a new sauropod dinosaur from the Morrison Formation (Upper Jurassic/Lower Cretaceous) of New Mexico, USA. *Journal of Vertebrate Paleontology*, **11**, 417–433.

Gilmore, C. W. 1932. On a newly mounted skeleton of *Diplodocus* in the United States National Museum. *Proceedings of the United States National Museum*, **81**, 1–21.

Gilmore, C. W. 1936. Osteology of *Apatosaurus*: with special reference to specimens in the Carnegie Museum. *Memoirs of the Carnegie Museum*, **11**, 175–300.

Gow, C. E. 1990. Morphology and growth of the *Massospondylus* braincase (Dinosauria, Prosauropoda). *Palaeontologia Africana*, **27**, 59–75.

Harris, J. D. 2006a. Cranial osteology of *Suuwassea emilieae* (Sauropoda: Diplodocoidea: Flagellicaudata) from the Upper Jurassic Morrison Formation of Montana, USA. *Journal of Vertebrate Paleontology*, **26**, 88–102.

Harris, J. D. 2006b. The axial skeleton of the dinosaur *Suuwassea emilieae* (Sauropoda: Flagellicaudata) from the Upper Jurassic Morrison Formation of Montana, USA. *Palaeontology*, **49**, 1091–1121.

Harris, J. D. 2006c. The significance of *Suuwassea emilieae* (Dinosauria: Sauropoda) for flagellicaudatan intrarelationships and evolution. *Journal of Systematic Palaeontology*, **4**, 185–198.

Harris, J. D. & **Dodson, P.** 2004. A new diplodocoid sauropod dinosaur from the Upper Jurassic Morrison Formation of Montana, USA. *Acta Palaeontologica Polonica*, **49**, 197–210.

Hatcher, J. B. 1901. *Diplodocus* (Marsh): its osteology, taxonomy, and probable habits, with a restoration of the skeleton. *Memoirs of the Carnegie Museum*, **1**, 1–61.

Hatcher, J. B. 1903. Osteology of *Haplocanthosaurus*, with description of a new species and remarks on the probable habits of the Sauropoda and the age and origin of the Atlantosaurus beds. *Memoirs of the Carnegie Museum*, **2**, 1–72.

Holland, W. J. 1906. The osteology of *Diplodocus* Marsh. *Memoirs of the Carnegie Museum*, **2**, 225–264.

Holland, W. J. 1915. A new species of *Apatosaurus*. *Annals of the Carnegie Museum*, **10**, 143–145.

Holland, W. J. 1924. The skull of *Diplodocus*. *Memoirs of the Carnegie Museum*, **9**, 378–403.

Ikejiri, T. 2012. Histology-based morphology of the neurocentral synchondrosis in *Alligator mississippiensis* (Archosauria, Crocodylia). *The Anatomical Record*, **295**, 18–31.

Ikejiri, T., **Tidwell, V.** & **Trexler, D. L.** 2005. New adult specimens of *Camarasaurus lentus* highlight ontogenetic variation within the species. Pp. 154–179 in V. Tidwell & K. Carpenter (eds) *Thunder-lizards: the Sauropodomorph dinosaurs*. Indiana University Press, Bloomington.

Janensch, W. 1929. Die Wirbelsäule der Gattung *Dicraeosaurus*. *Palaeontographica*, **2** (Supplement 7), 38–133.

Janensch, W. 1935. Die Schädel der Sauropoden *Brachiosaurus*, *Barosaurus* und *Dicraeosaurus* aus den Tendaguruschichten Deutsch-Ostafrikas. *Palaeontographica*, **2** (Supplement 7), 145–298.

Janensch, W. 1950. Die Wirbelsäule von *Brachiosaurus brancai*. *Palaeontographica*, **3** (Supplement 7), 27–93.

Jensen, J. A. 1985. Three new sauropod dinosaurs from the Upper Jurassic of Colorado. *Great Basin Naturalist*, **45**, 697–709.

Knoll, F., **Witmer, L. M.**, **Ortega, F.**, **Ridgely R. C.** & **Schwarz-Wings, D.** 2012. The braincase of the basal sauropod dinosaur *Spinophorosaurus* and 3D reconstructions of the cranial endocast and inner ear. *PLoS ONE*, **7**(1), e30060. DOI:10.1371/journal.pone.0030060

Kvale, E. P., **Hasiotis, S. T.**, **Mickelson, D. L.** & **Johnson, G. D.** 2001. Middle and Late Jurassic dinosaur fossil-bearing horizons: implications for dinosaur paleoecology, northeastern Bighorn Basin, Wyoming. *Guidebook for the Field Trips: Museum of the Rockies Occasional Paper*, **3**, 16–45.

Lovelace, D. M., **Hartman, S. A.** & **Wahl, W. R.** 2007. Morphology of a specimen of Supersaurus (Dinosauria, Sauropoda) from the Morrison Formation of Wyoming, and a re-evaluation of diplodocid phylogeny. *Arquivos do Museu Nacional Rio de Janeiro*, **65**, 527–544.

Lucas, S. G., **Spielmann, J. A.**, **Rinehart, L. F.**, **Heckert, A. B.**, **Herne, M. C.**, **Hunt, A. P.**, **Foster, J. R.** & **Sullivan, R. M.** 2006. Taxonomic status of *Seismosaurus hallorum*, a Late Jurassic sauropod dinosaur from New Mexico. *New Mexico Museum of Natural History and Science Bulletin*, **36**, 149–161.

Lull, R. S. 1919. The sauropodous dinosaur *Barosaurus* Marsh. *Memoirs of the Connecticut Academy of Arts and Sciences*, **6**, 1–42.

Madsen, J. H., **McIntosh, J. S.** & **Berman, D. S.** 1995. Skull and atlas-axis complex of the Upper Jurassic sauropod *Camarasaurus* Cope (Reptilia: Saurischia). *Bulletin of Carnegie Museum of Natural History*, **31**, 1–115.

Maidment, S. C. R. & **Porro, L. B.** 2010. Homology of the palpebral and origin of supraorbital ossifications in ornithischian dinosaurs. *Lethaia*, **43**, 95–111.

Mannion, P. D. 2011. A reassessment of *Mongolosaurus haplodon* Gilmore, 1933, a titanosaurian sauropod dinosaur from the Early Cretaceous of Inner Mongolia, People's Republic of China. *Journal of Systematic Palaeontology*, **9**, 355–378.

Mannion, P. D., **Upchurch, P.**, **Mateus, O.**, **Barnes, R.** & **Jones, M. E. H.** 2012. New information on the anatomy and systematic position of *Dinheirosaurus lourinhanensis* (Sauropoda: Diplodocoidea) from the Late Jurassic of Portugal, with a review of European diplodocoids. *Journal of Systematic Palaeontology*, **10**, 521–551. DOI:10.1080/14772019.2011.595432

Marsh, O. C. 1877. Notice of some new dinosaurian reptiles from the Jurassic Formation. *American Journal of Science, Series 3*, **14**, 514–516.

Marsh, O. C. 1878. Principal characters of American Jurassic dinosaurs, Part I. *American Journal of Science, Series 3*, **16**, 411–416.

Marsh, O. C. 1879. Notice of new Jurassic reptiles. *American Journal of Science, Series 3*, **18**, 510–505.

Marsh, O. C. 1884. Principal characters of American Jurassic dinosaurs. Part VII. On the Diplodocidae, a new family of the Sauropoda. *American Journal of Science, Series 3*, **27**, 160–168.

Marsh, O. C. 1890. Description of new dinosaurian reptiles. *American Journal of Science, Series 3*, **39**, 81–86.

McIntosh, J. S. 1990. Species determination in sauropod dinosaurs with tentative suggestions for their classification. Pp. 53–69 in K. Carpenter & P. J. Currie (eds) *Dinosaur Systematics: Perspectives and Approaches*. Cambridge University Press, New York.

McIntosh, J. S. 2005. The Genus *Barosaurus* Marsh (Sauropoda, Diplodocidae). Pp. 38–77 in V. Tidwell & K. Carpenter (eds) *Thunder-lizards: the Sauropodomorph dinosaurs*. Indiana University Press, Bloomington.

McIntosh, J. S. & **Berman, D. S.** 1975. Description of the palate and lower jaw of the sauropod dinosaur *Diplodocus* (Reptilia: Saurischia) with remarks on the nature of the skull of *Apatosaurus*. *Journal of Paleontology*, **49**, 187–199.

McIntosh, J. S., **Coombs, W. P.** & **Russell, D. A.** 1992. A new diplodocid sauropod (Dinosauria) from Wyoming, USA. *Journal of Vertebrate Paleontology*, **12**, 158–167.

McIntosh, J. S., **Miles, C. A.**, **Cloward, K. A.** & **Parker, J. R.** 1996. A new nearly complete skeleton of *Camarasaurus*. *Bulletin of the Gunma Museum of Natural History*, **1**, 1–87.

Michelis, I. 2004. *Taphonomie des Howe Quarry's (Morrison-Formation, Oberer Jura), Bighorn County, Wyoming, USA*. Unpublished PhD thesis, Institute of Palaeontology, University of Bonn, 41 pp.

Osborn, H. F. 1899. A skeleton of *Diplodocus*. *Memoirs of the American Museum of Natural History*, **5**, 191–214.

Osborn, H. F. & **Mook, C. C.** 1921. *Camarasaurus*, *Amphicoelias*, and other sauropods of Cope. *Memoirs of the American Museum of Natural History, New Series*, **3**, 249–387.

Owen, R. 1842. Report on British Fossil Reptiles Pt. II. *Report of the British Association for the Advancement of Science*, **1841**, 60–204.

Peterson, O. A. & **Gilmore, C. W.** 1902. *Elosaurus parvus*; a new genus and species of the Sauropoda. *Annals of the Carnegie Museum*, **1**, 490–499.

Reisz, R. R., **Scott, D.**, **Sues, H.-D.**, **Evans, D. C.** & **Raath, M. A.** 2005. Embryos of an Early Jurassic prosauropod dinosaur and their evolutionary significance. *Science*, **309**, 761–764.

Remes, K. 2006. Revision of the Tendaguru sauropod dinosaur *Tornieria africana* (Fraas) and its relevance for sauropod paleobiogeography. *Journal of Vertebrate Paleontology*, **26**, 651–669.

Remes, K. 2007. A second Gondwanan diplodocid dinosaur from the Upper Jurassic Tendaguru beds of Tanzania, East Africa. *Palaeontology*, **50**, 653–667.

Remes, K. 2009. Taxonomy of Late Jurassic diplodocid sauropods from Tendaguru (Tanzania). *Fossil Record*, **12**, 23–46.

Salgado, L. & **Bonaparte, J. F.** 1991. Un nuevo saurópodo Dicraeosauridae, *Amargasaurus cazaui* gen. et sp. nov., de la Formación La Amarga, Neocomiano de la provincia del Neuquén, Argentina. *Ameghiniana*, **28**, 333–346.

Schwarz, D., **Frey, E.** & **Meyer, C. A.** 2007a. Pneumaticity and soft-tissue reconstructions in the neck of diplodocid and dicraeosaurid sauropods. *Acta Palaeontologica Polonica*, **52**, 167–188.

Schwarz, D., **Ikejiri**, **T., Breithaupt**, **B. H., Sander**, **P. M.** & **Klein**, **N.** 2007b. A nearly complete skeleton of an early juvenile diplodocid (Dinosauria: Sauropoda) from the Lower Morrison Formation (Late Jurassic) of north central Wyoming and its implications for early ontogeny and pneumaticity in sauropods. *Historical Biology*, **19**, 225–253.

Sereno, P. C., **Wilson, J. A.**, **Witmer, L. M.**, **Whitlock, J. A.**, **Maga, A.**, **Ide, O.** & **Rowe, T. A.** 2007. Structural extremes in a Cretaceous dinosaur. *PloS ONE*, **2**, e1230.

Sternfeld, R. 1911. Zur Nomenklatur der Gattung *Gigantosaurus* Fraas. *Sitzungsberichte der Gesellschaft Naturforschender Freunde zu Berlin*, **1911**, 398.

Swierc, J. E. & **Johnson, G. D.** 1996. A local chronostratigraphy for the Morrison Formation, northeastern Bighorn Basin, Wyoming. Pp. 315–327 in C. E. Bowen, S. C Kirkwood & T. S Miller (eds) *Resources of the Bighorn Basin: Forty-seventh annual field conference guidebook*. Wyoming Geological Association, Casper.

Tang, F., **Jing, X.**, **Kang, X.** & **Zhang, G.** 2001. *Omeisaurus maoianus: a complete sauropod from Jingyuan, Sichuan*. China Ocean Press, Beijing. [In Chinese with English summary].

Taylor, M. P. & **Naish**, **D.** 2005. The phylogenetic taxonomy of Diplodocoidea (Dinosauria: Sauropoda). *PaleoBios*, **25**(2), 1–7.

Trujillo, K. C. 2006. Clay mineralogy of the Morrison Formation (Upper Jurassic - ?Lower Cretaceous), and its use in long distance correlation and paleoenvironmental analyses. *New Mexico Museum of Natural History and Science Bulletin*, **36**, 17–23.

Turner, C. E. & **Peterson, F.** 1999. Biostratigraphy of dinosaurs in the Upper Jurassic Morrison Formation of the Western Interior, USA. Pp. 77–114 in D. D. Gillette (ed.) *Vertebrate Paleontology in Utah*. Utah Geological Survey Miscellaneous Publication, Salt Lake City.

Upchurch, P. 1995. The evolutionary history of sauropod dinosaurs. *Philosophical Transactions of the Royal Society of London. Series B*, **349**, 365–390.

Upchurch, P. 1998. The phylogenetic relationships of sauropod dinosaurs. *Zoological Journal of the Linnean Society*, **124**, 43–103.

Upchurch, P. & **Mannion**, **P. D. 2009**. The first diplodocid from Asia and its implications for the evolutionary history of sauropod dinosaurs. *Palaeontology*, **52**, 1195–1207.

Upchurch, P., **Barrett, P. M.** & **Dodson, P.** 2004a. Sauropoda. Pp. 259–322 in D. B. Weishampel, P. Dodson & H. Osmólska (eds) *The Dinosauria.* Second edition. University of California Press, Berkeley.

Upchurch, P., **Tomida, Y.** & **Barrett, P. M.** 2004b. A new specimen of *Apatosaurus ajax* (Sauropoda: Diplodocidae) from the Morrison Formation (Upper Jurassic) of Wyoming, USA. *National Science Museum Monographs*, **26**, 1–108.

Varricchio, D. J. 1997. Growth and embryology. Pp. 282–288 in P. J. Currie & K. Padian (eds) *Encyclopedia of Dinosaurs*. Academic Press, London.

Wedel, M. J. & **Sanders, R. K.** 2002. Osteological correlates of cervical musculature in Aves and Sauropoda (Dinosauria: Saurischia), with comments on the cervical ribs of *Apatosaurus*. *PaleoBios*, **22**(3), 1–6.

Wedel, M. J., **Cifelli, R. L.** & **Sanders, R. K.** 2000. Osteology, paleobiology, and relationships of the sauropod dinosaur *Sauroposeidon*. *Acta Palaeontologica Polonica*, **45**, 343–388.

Whitlock, J. A. 2011a. A phylogenetic analysis of Diplodocoidea (Saurischia: Sauropoda). *Zoological Journal of the Linnean Society*, **161**, 872–915.

Whitlock, J. A. 2011b. Inferences of diplodocoid (Sauropoda: Dinosauria) feeding behavior from snout shape and microwear analyses. *PloS ONE*, **6**(4), e18304.

Whitlock, J. A. 2011c. Re-evaluation of *Australodocus bohetii*, a putative diplodocoid sauropod from the Tendaguru Formation of Tanzania, with comment on Late Jurassic sauropod faunal diversity and palaeoecology. *Palaeogeography, Palaeoclimatology, Palaeoecology*, **309**, 333–341.

Whitlock, J. A. & **Harris, J. D.** 2010. The dentary of *Suuwassea emilieae* (Sauropoda: Diplodocoidea). *Journal of Vertebrate Paleontology*, **30**, 1637–1641.

Whitlock, J. A., **Wilson, J. A.** & **Lamanna, M. C.** 2010. Description of a nearly complete juvenile skull of *Diplodocus* (Sauropoda: Diplodocoidea) from the Late Jurassic of North America. *Journal of Vertebrate Paleontology*, **30**, 442–457.

Wilborn, B. K. 2008. *Paleoecology and stratigraphy of the Morrison and Cloverly Formations, Bighorn Basin, Wyoming*. Unpublished PhD Dissertation, Conocophillips School of Geology and Geophysics, University of Oklahoma, 291 pp.

Wilson, J. A. 1999. A nomenclature for vertebral laminae in sauropods and other saurischian dinosaurs. *Journal of Vertebrate Paleontology*, **19**, 639–653.

Wilson, J. A. 2002. Sauropod dinosaur phylogeny: critique and cladistic analysis. *Zoological Journal of the Linnean Society*, **136**, 215–275.

Wilson, J. A. 2005. Overview of sauropod phylogeny and evolution. Pp. 15–49 in K. A. Curry Rogers & J. A. Wilson (eds) *The Sauropods: Evolution and Paleobiology*. University of California Press, Berkeley.

Wilson, J. A., **D'Emic, M. D.**, **Ikejiri, T.**, **Moacdieh, E. M.** & **Whitlock, J. A.** 2011. A nomenclature for vertebral fossae in sauropods and other saurischian dinosaurs. *PLoS ONE*, **6** (2), e17114.

Wilson, J. A. & **Sereno, P. C.** 1998. Early evolution and higher-level phylogeny of sauropod dinosaurs. *Journal of Vertebrate Paleontology*, **18** (Supplement 2), 1–79.

Wilson, J. A. & **Smith, M. B.** 1996. New remains of *Amphicoelias* Cope (Dinosauria: Sauropoda) from the Upper Jurassic of Montana and diplodocid phylogeny. *Journal of Vertebrate Paleontology*, **16** (Supplement), 73A.

Wilson, J. A. & **Upchurch, P.** 2009. Redescription and reassessment of the phylogenetic affinities of *Euhelopus zdanskyi* (Dinosauria: Sauropoda) from the Early Cretaceous of China. *Journal of Systematic Palaeontology*, **7**, 199–239.

Woodruff, C. & **Fowler, D. W.** 2012. Ontogenetic influence on neural spine bifurcation in diplodocoidea (Dinosauria: Sauropoda): A critical phylogenetic character. *Journal of Morphology*, **273**, 754–764.